Journal of Environmental Chemical Engineering 10 (2022) 107811

Contents lists available at ScienceDirect

Journal of Environmental Chemical Engineering

journal homepage: www.elsevier.com/locate/jece

Electrospun polyurethane nanofibers coated with polyaniline/polyvinyl alcohol as ultrafiltration membranes for the removal of ethinylestradiol hormone micropollutant from aqueous phase

Muhammad Yasir *, Fahanwi Asabuwa Ngwabebhoh, Tomáš Šopík, Hassan Ali, Vladimír Sedlařík *

Centre of Polymer Systems, University Institute, Tomas Bata University in Zlín, Třída Tomáše Bati 5678, 76001 Zlín, Czech Republic

ARTICLE INFO

Editor: Pei Xu

Keywords:
Hormone removal
Electrospun nanofibers
in situ coating
Adsorption
Water remediation

ABSTRACT

Estrogenic hormones at significant levels are a serious cause of fish femininity, breast and ovarian cancer as a consequence of hormonal imbalance. This study reports the fabrication of electrospun polyurethane (PU) nanofibers modified by coating with polyaniline/polyvinyl alcohol (PANI/PVA) to form filtration membranes for the enhanced removal of ethinylestradiol (EE2) estrogenic hormone. Structural and morphological characterization was performed by FTIR, SEM and optical microscopy, while the detection and quantification of EE2 were analysed using HPLC. To understand the material characteristics, the feasibility of the results based on contact time and kinetics to determine the adsorption capacity coated PU nanofibers was further investigated. Findings demonstrated that EE2 best fitted pseudo-second-order kinetics. Furthermore, the adsorption process was optimised via response surface methodology using a central composite design model by varying parameters such as pH, temperature, the concentration of adsorbate, and adsorbent dosage to determine. It was found that the modified PU membranes had a maximum adsorption capacity of 2.11 mg/g and high removal percentage efficiency of ~82.20% for EE2. Adsorption mechanism and thermodynamics were also evaluated, and the results depicted the adsorption process of EE2 occurred via intraparticle diffusion and was exothermic in nature. Finally, a reusability study was done over six adsorption-desorption cycles to test the consistent effectiveness of the modified PU membrane, which remained above 80% removal capacity. Overall, the findings indicate that treated PU with stabilized PANI particles possess the potential to form an effective adsorbent for eradicating EE2 and other estrogenic hormones from the environment.

1. Introduction

In the last few decades, rapid industrialization and human population growth have raised serious environmental concerns due to the high demand for various synthetic chemicals, which are being released into the environment without proper treatment. These synthetic chemicals contain micropollutants as by-products that tend to pose grave risks to animals and humans, thereby threatening the planet's ecosystem. Amongst all, discharged micropollutants from the pesticide and pharmaceutical industry are of special interest due to their relatively high bio-toxicity. The commonly discharged micropollutants are steroidal hormones such as estrogen, testosterone, estrone, ß-estradiol, ethinylestradiol, and estriol that possess bio-potency even at sub nanogram scale [1–3]. These micropollutants along with other synthetically produced chemicals such as bisphenols and polyfluoroalkyl are known as endocrine-disrupting chemicals (EDCs) due to their adverse interaction with the endocrine system [4–6]. They circulate in the body and are released into the blood via the endocrine system as a primary response to hunger, starvation, obesity, and other physiological functions. The presence of any EDC leads to impairment in many important bodily functions vital for maintaining a healthy body [7]. So far, the scientific consensus is clear about the growing incidence rate of several diseases such as reproductive problems, leukaemia, brain cancer, and neurological disorders associated with exposure to EDCs [6]. Therefore, to alleviate the risk of EDCs, several major health and regulatory institutions around the world have established a threshold level for the concentration of contaminants present in drinking water. Recently, the European Union directive 2020/2184 concerning the quality of drinking

* Corresponding authors.
E-mail addresses: yasir@utb.cz (M. Yasir), sedlarik@utb.cz (V. Sedlařík).

https://doi.org/10.1016/j.jece.2022.107811
Received 31 January 2022; Received in revised form 19 April 2022; Accepted 25 April 2022
Available online 28 April 2022

water recommended a threshold limit of 1 ng/L as a benchmark for assessing the occurrence and treatment of EDCs [8].

Ethinylestradiol (EE2) is one of the most commonly occurring synthetic steroid due to its extensive use in contraceptive pills and treatment of sexual dysfunctions in females [9]. Unlike the naturally released estradiol, synthetically produced EE2 is 10–50 times more potent and has a high degree of bioaccumulation in vertebrates. Therefore, proper environmental remediation and removal of EE2 has been of main research goal due to relatively high adverse effects on the bio-ecosystems [10]. Over the past few years, EE2 concentration in fresh water resources has been rising gradually as conventional waste water treatment plants are ineffective for the total or partial removal of EE2. To address this problem, several strategies have been implemented to remediate this hormone EE2 as a micropollutant alongside other related environmentally persistent toxicants. Different treatment techniques such as biological degradation, advanced oxidation process, catalytic reduction, photocatalysis, and adsorption method have been investigated [11–19]. Out of these methods, the elimination of EDCs by adsorption process has proven to be more beneficial due to low concentration target compounds, simplicity, and cost-effectiveness [20]. Moreover, the formation of toxic by-products is avoided, which are generated in the case of other conventional techniques. The removal of EDCs by highly adsorbent materials such as activated carbon, carbonaceous materials, biochar, etc., have been investigated [21–23]. However, these materials pose a risk of secondary pollution due to difficult separation from the solution and are usually discarded after limited usage [24]. To resolve this issue, polymer-based nanofibers have been recently investigated with a high degree of recyclability and water permeability, demonstrating their potential for practical application compared to conventional membranes [25,26].

Electrospinning is the most common process by which ultrafine nanofibers in precisely controlled conditions can be fabricated, having small pore size distribution, high surface area, and increased surface flexibility [27,28]. In addition, this technique allows ease in modification of the prepared materials by incorporation of additional components with functionalized properties to achieve higher performance [29]. So far, various types of polymers have been used for fabricating electrospun nanofibers, such as polyacrylonitrile, cellulose acetate, polyamide, and polyvinylidene fluoride [30–34]. Depending on the targeted type of pollutant, additional functional molecules have been introduced in the fibrous matrix, such as polydiacetylene, Au/Ag nanoparticles, Schiff base, polyethyleneimine, and rhodamine derivatives [35–38]. However, post modification of these spun nanofibers to enhance functionality properties with high nitrogen containing compounds is limited. This process has proven to greatly enhance adsorption performance for different persistent environmental pollutants [39,40]. Polyaniline (PANI) is a widely used conducting and electroactive polymer due to its cost-effective synthesis via either simple chemical or electrochemical oxidation [41,42]. This conductive polymer possessed benzenoid and quinonoid rings in its structural units linked by amine- and/or imine-type nitrogen atoms via π–π interactions and hydrogen bonding [43,44]. This makes PANI and its related composite materials promising adsorbents of organic pollutants. However, PANI in combination with supporting polymers such as polyvinyl alcohol, can enhance the materials both with appreciable electrical conductivity and mechanical integrity [45]. In water pollution treatment, the incorporation of such polymer in the adsorbent material increases the presence of nitrogen atoms, which in turn enhances the ability to interact with pollutants via formation of complexes with various organic and inorganic substances to reduce their prevalence in the aqueous phase.

In this study, polyurethane (PU) membranes are prepared via electrospinning and further post modified by coating with polyaniline in a polyvinyl alcohol solution for the enhanced removal of EE2 micropollutant hormone. To understand the characteristics of the coated PU membranes, FTIR, SEM, and optical microscopy were performed. The adsorptive interaction and performance for the removal of EE2 were further investigated via optimization study using response surface methodology to evaluate the experimental data by analysis of variance (ANOVA) to determine optimum adsorption capacity via adsorptive two parameters interactions. Furthermore, we validated the determined optimal adsorption condition by studying effects on single parameters of solution pH, temperature, initial concentration of the hormone, and adsorbent dosage. Kinetics and thermodynamics of the adsorption process were also calculated. Finally, a reusability analysis of the prepared adsorbent over six adsorption-desorption cycles was performed in order to determine the consistent effectiveness of coated PU membrane.

2. Materials and methods

2.1. Materials and reagents

17α-ethinylestradiol (EE2, ≥98%) as the model estrogenic hormone, 4,4′-methylene-diphenyl diisocyanate (MDI), (poly 3-methyl-1,5-pentanediol-alt-adipic, isophthalic acid) (PAIM),1,4 butanediol (BD), aniline (≥99% purity), hydrochloric acid, (HCl, 37% purity), ammonium peroxydisulfate, poly(vinyl alcohol) (Mowiol 20–98, molecular weight 125,000) and ammonium hydroxide (28–30% NH_3 basis) were purchased from Sigma-Aldrich, Germany. Sodium tetra-borate decahydrate (borax) and citric acid were purchased from PENTA s.r.o., N,N-dimethylformamide (DMF >99.5%) from Lach-Ner, s.r.o, Acetonitrile (HPLC grade) from Honeywell and ethanol (HPLC grade > 99%) from VWR, Czech Republic. Deionized water (pH 7, 18.2 MΩ/cm) was prepared in a laboratory Milli-Q ultrapure (Type 1) water purification system (Biopak® Polisher, Merck, USA) and used for preparation/purification purposes.

2.2. Fabrication of nanofibers

2.2.1. Step 1: preparation of polymer solution

Polyurethane (PU), also known as PU918, was prepared by a polyaddition reaction in the Centre of Polymer Systems (CPS), Zlin, Czech Republic). Initially, MDI, PAIM polymer diol ($Mw = 2 \times 10^3$ g/mol), and BD in a molar ratio 9:1:8 were synthesized at 90 °C for 5 h (per parts way of the synthesis). The preparation of a pre-polymer started with MDI and PAIM as precursors, followed by the addition of BD and MDI in appropriate amounts. Then, 13 wt% of prepared polyurethane with $Mw = 9.8 \times 10^4$ g/mol was dissolved in DMF. A separate solution of borax and citric acid (BC) was prepared in a ratio of 1:3, respectively. Then, 35 wt% of BC was dissolved in DMF solution and agitated in a mixer for 5 h at 400 rpm. The electrical conductivity of PU solution was adjusted and optimized to ideal by supplementing with BC solution prior to electrospinning [46].

2.2.2. Step 2: electrospinning process for the production of PU nanofibers

The nanofiber layers were prepared from PU solutions in DMF with a spin line machine in CPS, equipped with a patented rotating electrostatic electrode with nanofibers forming jets (CZ305037; PCT/CZ2010/000042). A schematic illustration of the electrospinning system is illustrated in Scheme 1. The optimum experimental conditions to produce free of defect PU nanofiber membranes were as follows: electric voltage applied to PU solution: 75 kV, PU solution dosing: 0.24 mL/min, relative humidity: 30%, temperature: 22 ± 2 °C, the distance between electrodes: 18 cm, rotational speed of supporting polypropylene (PP) fabric sheet collecting nanofibers: 16 cm/min, and dimension of polypropylene (PP) roll collector: 40 cm of width.

2.3. Post-modification of spun PU nanofiber membrane

Polyaniline (PANI) stabilized with poly(vinyl alcohol) (PVA) system was prepared by the oxidation of aniline in hydrochloride with ammonium peroxydisulfate as previously described [46,47] with slight modifications. In brief, aniline (0.1 M) dissolved in 1 M HCL solution was

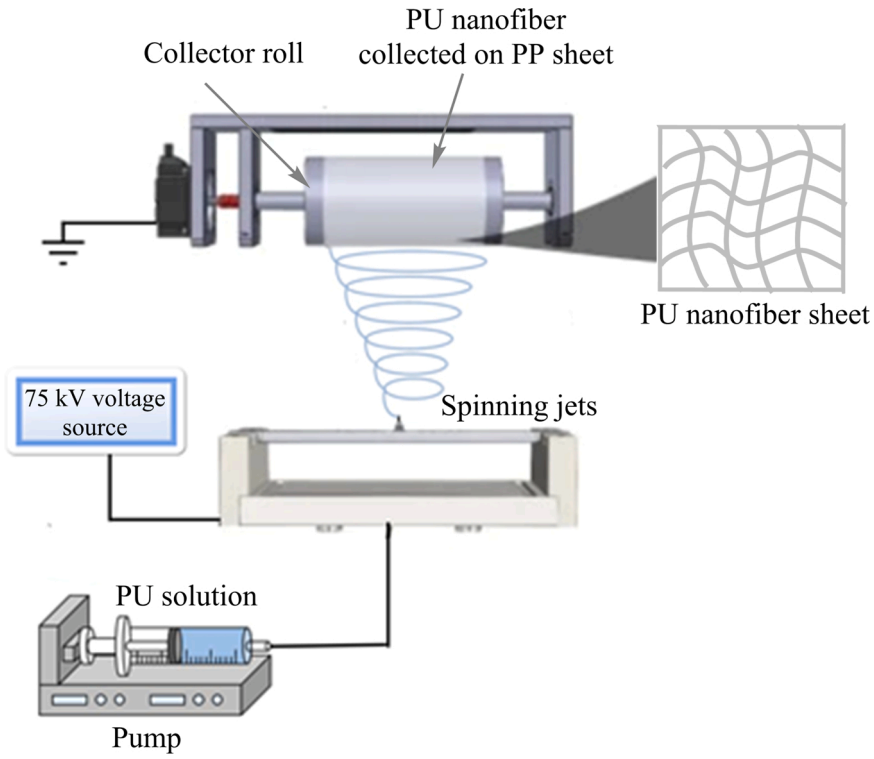

Scheme 1. Illustration of the electrospinning system for the production of the PU nanofiber sheets.

mixed with 4 wt% aqueous solution of PVA to form a 50 mL solution. Weighed 0.5 g spun PU nanofiber was dipped in the above prepared solution for 2 h to allow for the adsorption of the aniline monomer on the surface of the fibers. An equal volume (50 mL) of 0.125 M of ammonium peroxydisulfate solution was added to the mixture, shortly stirred, and allowed at room temperature for 24 h for the polymerization of aniline to occur and coating on the spun fibers. The originally white solution turned dark green/black as PANI was produced. The coated spun fibers were then removed and repeatedly re-suspended in 0.2 M HCL to remove residual or unreacted monomers, followed by washing severally with distilled water to neutral pH. The coated sample known as PU-PANI emeraldine salt (PU-PANI-ES) was subsequently freeze-dried for further use. PU-PANI-ES was further converted to PU-PANI emeraldine base (PU-PANI-EB) by suspension of the coated membranes in excess 1 M ammonium hydroxide for 24 h [48]. Thus, blue PANI base coated PU nanofibrous membranes were collected by filtering the residual solution, washed with acetone and water repeatedly, then dried as above.

2.4. Characterization technique

2.4.1. Fourier-transform infrared spectroscopy (FTIR)

FTIR analysis was conducted on a Nicolet 320 spectrometer (ThermoScientific, USA), equipped with Ge crystal to identify the functional groups present on the treated and control PU nanofiber membranes. Attenuated total reflectance (ATR) spectra were recorded across 400−4000 cm^{-1} under standard conditions. The resolution was set to 4 cm^{-1} and the scan rate to 64.

2.4.2. Optical microscopy

Imaging under an optical microscope was collected with a digital microscope of high degree magnification Leica DVM2500 (Leica Microsystems, Czech Republic) in order to observe the coated PU nanofibrous membranes. Visualization was performed under phase contrast mode, which allows visibility of the coated membranes. Imaging was observed at 100x magnification.

2.4.3. Scanning electron microscopy

Micro images were recorded to witness the surface morphology of the fibers on a Nova 450 scanning electron microscope (SEM) (FEI, Thermo Fisher Scientific, USA). Also, the desired fiber diameter and any sort of defects, for instance, beads in the structure, were checked at the acceleration voltage of 5−10 kV via a through-the-lens detector (TLD).

2.4.4. High-performance liquid chromatography (HPLC) analysis

Standard calibration of EE2 hormone and concentration measurement of samples was performed on an HPLC DionexUltiMate 3000 Series (Thermo Fisher Scientific, Germany). A reversed-phase column (Kinetex 2.6 u C18 100 A (150 ×4.6 mm; Phenomenex, USA)) guarded with a security column (Phenomenex, USA) was used for the separation at 30 °C. The mobile phase was a mixture of acetonitrile and water in a ratio (45:55, v/v), and the flow rate was set to 0.8 mL/min under isocratic mode for a total run time of 12 min 20 μL of testing volume was injected onto the column from the sampler chamber at 5 °C. The EE2 hormone elute concentrations were detected and quantified at a wavelength of 200 nm.

2.5. Adsorption experimental design

Batch static adsorption was performed to determine the removal capacity of investigated coated spun PU nanofiber membranes. 100 mL hormone solutions in 250 mL conical flasks were used to investigate the adsorption efficiency. The flasks were under continuous shaking on an orbital incubator shaker (Stuart® S1500, Barloworld Scientific Ltd., UK) at 250 rpm by varying different parameters of initial concentration of hormone (mg/L), solution pH, adsorbent dosage (mg), and temperature of adsorbate solution (°C). At predetermined time intervals, 4 mL of residual solution was collected, followed by readings performed in triplicate and the average values recorded. The equilibrium adsorption capacity and removal percentages of the hormone were then determined using the mathematical Eqs. (1) and (2), respectively [46,49].

$$Hormone \quad uptake(q_e) = v \times \frac{(C_i - C_e)}{M} \tag{1}$$

$$Hormone \quad removal \quad (\%) = \frac{C_i - C_t}{C_i} \times 100 \tag{2}$$

where C_i is the initial concentration (mg/L), and C_t is the concentration of the solution at time t (mg/L). M is the mass of adsorbent (g), V is the volume of solution (L), and q_e is equal to the equilibrium adsorption capacity (mg/g).

Central Composite Design (CCD) model was employed using the Design-Expert software v13.0 to estimate and optimize the most influencing factors and their interaction effects on EE2 hormone removal by the coated spun PU nanofiber membranes. CCD is composed of factorial points corresponding to axial and central points [50,51]. The levels of the main investigated factors are given in Table 1. The relationship between these independent factors based on the obtained responses is fitted to a second-order polynomial equation that allows for the modelling of responses of the hormone, which is expressed by Eq. (3).

$$Y = \beta_o + \sum_{i=1}^{k} \beta_i X_i + \sum_{i=1}^{k} \beta_{ii} X_i^2 + \sum_{i=1}^{k} \sum_{j=i+1}^{k} \beta_{ij} X_i X_j + \varepsilon \tag{3}$$

Where Y is the response (removal efficiency), X_i and X_{ij} are the encoded parameters, and β_0, β_i, β_{ii}, and β_{ij} are the linear, quadratic, and interaction coefficients, respectively. Based on the results generated, the desirability function is then employed to obtain the optimization of investigated parameters (best levels for each factor).

2.6. Adsorption-desorption analysis

After adsorption, the adsorbent material was treated by desorption of the adsorbed EE2 hormone. For the desorption test, the PU adsorbents were extracted from the conical flasks containing the hormone solutions and washed with distilled water, followed by gentle stirring at a constant 100 rpm for 10 min in a 100 mL mixture of 1:1 water and ethanol to remove the hormones entirely and eluted in the aqueous phase. Then, the PU adsorbent was re-placed in 100 mL water until the next adsorption cycle. The procedure was repeated for six consecutive adsorption-desorption cycles. Readings were collected in triplicates, and the average value was recorded.

2.7. Statistical and error analysis

The data are displayed as Mean ± Standard error. OriginLab v.9.0 and Design expert software v.13.0 were used for statistical analysis. The difference between values was determined by a one-way analysis of variance (ANOVA). A value of $p < 0.05$ was determined as statistically significant. Error analysis parameters such as the determination coefficient (R^2) were used to ascertain the difference between the experimental and theoretical data. In addition, the sum of squared errors (*SSE*) and Chi-squared (χ^2) were employed to minimize errors since inherent bias occurs during the linearization of equations, such as in kinetic modelling.

Table 1
Investigated experimental factors and their levels in the central composite design.

Factors	Low (−1)	Center (0)	High (+1)
A – Temperature (°C)	25.00	40.00	55.00
B – Solution pH	5.00	7.00	9.00
C – Initial conc. of hormone (mg/L)	0.20	0.30	0.40
D – Adsorbent dosage (mg)	10.00	20.00	30.00

3. Results and discussion

3.1. Modification of spun nanofibers

PANI is typically achieved by the oxidation of aniline with ammonium peroxydisulfate in an acidic aqueous medium at room temperature, followed by deprotonation with ammonium hydroxide for PANI base (Scheme 2a). The treatment of the PU nanofibrous membrane with PANI serves as an alternative to improve the functional properties of materials. In order to obtain soft conducting and filtration membranes, another component, such as a water-soluble supporting polymer, in this case, PVA was incorporated into the system to enhance homogenous PANI being formed with low agglomeration and increase surface interaction with the PU fibers [46,52]. PVA, as a supporting polymer, forms a skeletal network between the PANI particles and PU fibers that further strengthens the integrity of the membrane [46]. Considering that PANI is produced in the vicinity of the PVA phase, where the reactants are gradually concentrated during polymerization and bind to the PU fiber surface to form PU-PANI-ES, which is then deprotonated to PU-PANI-EB in the basic medium (Scheme 2b and c). This leads to the formation of modified PU nanofibrous membranes rich in nitrogen atoms, which is composed of conducting and supporting polymer phases possessing a composite nature. This makes them suited as good adsorbents to be explored for the removal of micropollutants (such as estrogenic hormones) from the aqueous phase.

3.2. Material characterization

3.2.1. FTIR analysis

The FTIR spectra of neat PU, PU-PANI-ES, and PU-PANI-EB are presented in Fig. 1. The FTIR spectra of PU shows a broad peak between 3700 and 3200 cm^{-1} corresponds to the N-H bond stretching vibrations from the aliphatic amino group of carbamate. The peaks at 2952 and 2889 cm^{-1} reflect C-H asymmetrical flexing vibration of aliphatic CH_2 groups, respectively [53]. The strong absorption peak around 1710 cm^{-1} is ascribed to amido ester C═O stretching vibration [54,55]. The peaks at 1590 and 1522 cm^{-1} are attributed to the N-H bending of the amide group. The characteristic peaks arising at 1410 and 1307 cm^{-1} illustrate the stretching vibration in the skeleton of the benzene ring due to the C═C bond [56]. The stretching vibration peak at 1240 cm^{-1} relates to the C-N bond from the amide group. The asymmetric flexing vibration of C-O-C bonds is caused by alkyl ether and is represented by a sharp peak at 1080 cm^{-1} [46,57]. The peak at 708 and 730 cm^{-1} are attributed to aryl C-H bending. PVA did not show any obvious absorption band in the study, which may be attributed to overlapping its peak with PU.

The FT–IR spectra of PU-PANI-ES and PU-PANI-EB showed a characteristic broad band between 3700 and 3200 cm^{-1}, attributed to the overlapping stretching vibrations of N–H from PU, PANI, and OH from PVA. The peaks at about 1590 and 1522 cm^{-1} which showed increased intensity for coated PU materials with PANI are ascribed to the absorption of quinone and benzene rings of PANI [58]. The peaks at 1307 and 1136 cm^{-1} also depicted increased intensity for PANI coated PU materials and relates to the alkyl C–N stretching vibration from PU and PANI. The peak at 815 cm^{-1} further showed increased intensity for the PANI coated samples and is attributed to the π localized polaron band of coated PANI on PU fibers [59].

3.2.2. Optical microscopy

It is visible by the optical microscopy (Fig. 2) that the coated samples (either green or blue) provide good phase contrast while showing the fibrillary structure of the membranes. After freeze-drying, they convert to lightweight membranes. Considering the change in color of the PU membranes from white to green and blue confirms the coating of PANI on the fiber surface of PU during preparation. This makes the formed modified PU membranes suited to be exploited as novel adsorbents.

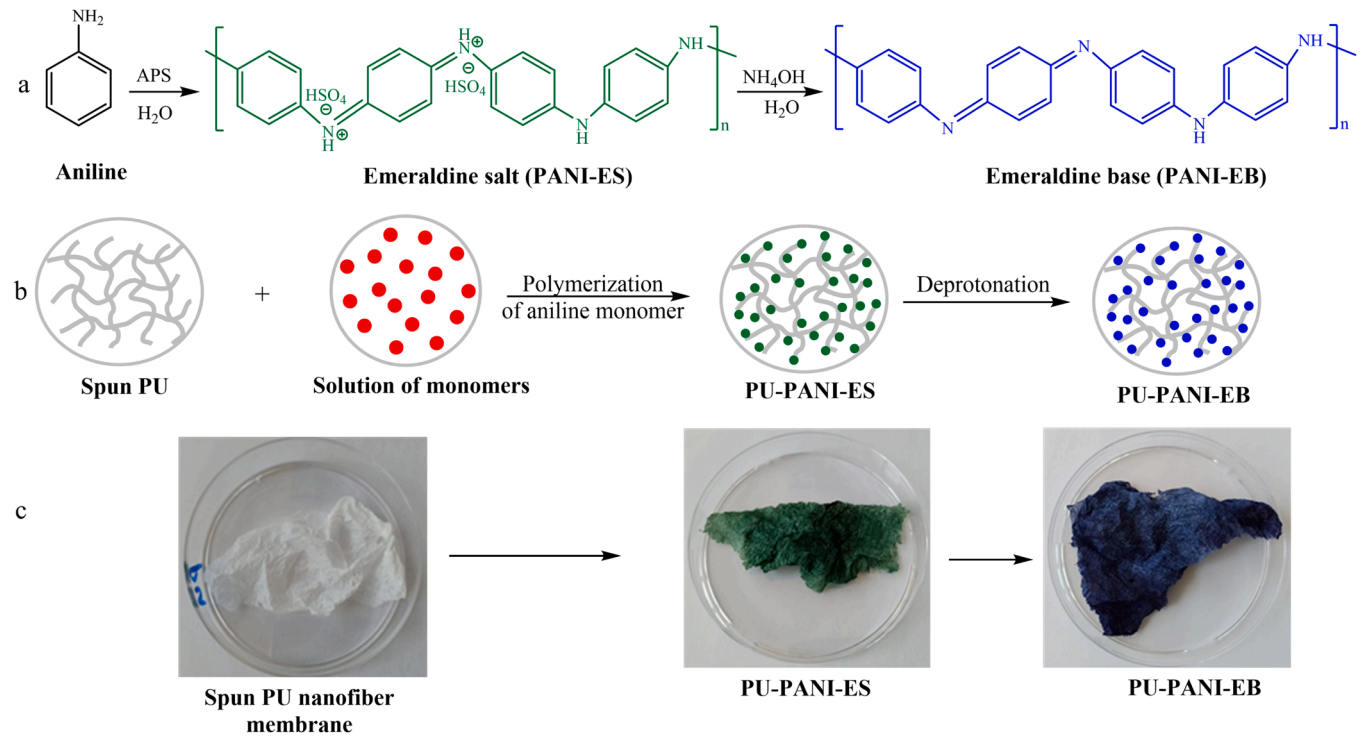

Scheme 2. (a) Aniline is oxidized to PANI (emeraldine) salt (PANI-ES) with ammonium peroxydisulfate and deprotonated to PANI (emeraldine) base (PANI-EB) using ammonium hydroxide. (b) Spun PU membrane (gray spirals) mixed with a solution of monomers (red circles) subsequently monomer polymerize to a polymer (green objects) and adhere to PU fiber surface. After that green PANI is deprotonated to an emeraldine base (blue objects). (c) Images of neat spun PU membrane, PU-PANI-ES and PU-PANI-EB coated membranes.

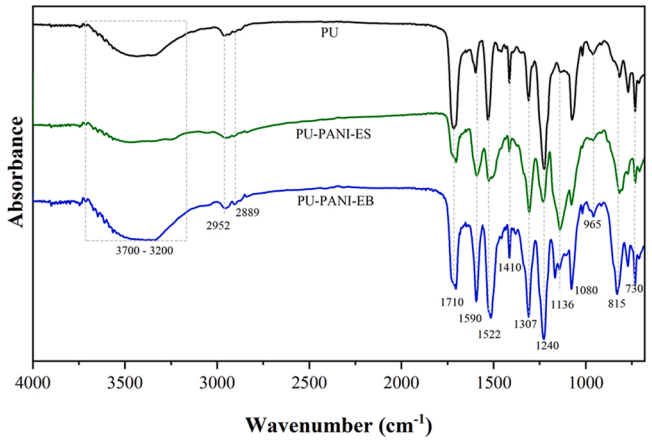

Fig. 1. FTIR spectra of neat PU as control, PU-PANI-ES, and PU-PANI-EB treated fibers from attenuated total reflectance (ATR) sampling.

3.2.3. SEM analysis

The micrographs in Fig. 3 show that the electrospun nanofiber of PU exhibit a minimum diameter of approximately 174 ± 56 nm, as previously reported by Yasir et al. [46]. These fibers, after treatment with PANI become more dense and thicker due to the adsorption of polymerized PANI particles on the surface of fibers. This makes the structure more compact, as seen in the case of PU-PANI-ES and PU-PANI-EB. However, PU-PANI-ES is more denser compared to PU-PANI-EB because the latter was further deprotonated, which may have resulted in the loss of some particles during treatment, making it less dense. Overall, both of the modified materials appear to have a better morphology compared to the PU control, and it is also proved further by the improvement in the performance of the materials shown in the following section.

3.3. Adsorption study

In order to test the efficiency of prepared materials as suitable adsorbents, a preliminary adsorption study was performed for neat PU and coated PU samples (PU-PANI-ES and PU-PANI-EB). Fig. 4 presents the results obtained from the experiment done with 20 mg of each adsorbent in 100 mL EE2 hormone solution with a concentration of 0.20 mg/L for 3.5 h at 150 rpm, room temperature, and pH 7. The results show that the coated PU materials with PANI significantly improved the adsorption of EE2. The neat PU had a removal efficiency and adsorption capacity of 55.38% (0.612 mg/g), which increased to 81.46% (0.900 mg/g), and 90.33% (0.998 mg/g) for PU-PANI-EB and PU-PANI-ES, respectively. Based on the achieved results, the best sample (PU-PANI-ES) was further studied via an optimization study to determine the optimum removal conditions for the EE2 hormone.

3.4. Batch adsorption optimization study

The optimum adsorption parametric conditions for the present study were determined by analysis of the obtained experimental data (Table 2) via CCD model using response surface methodology. The recorded experimental response values (removal capacity) were fitted to a second−order polynomial equation generated by the Design−Expert 9 software (Stat−Ease Inc., USA). Herein, 20 experimental runs were evaluated according to the response surface design method. Four operating factors were investigated in the optimization study, including temperature, solution pH, initial concentration of the hormone, and

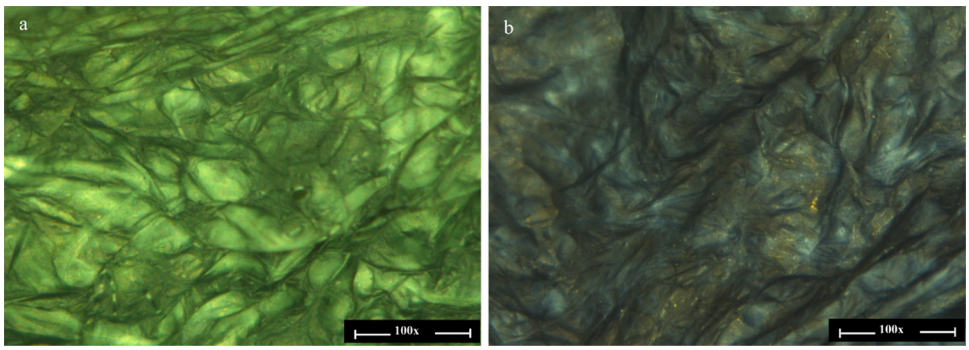

Fig. 2. Optical micrograph of coated (a) PU-PANI-ES and (b) PU-PANI-EB membranes at 100x magnification.

adsorbent dosage, coded as A, B, C, and D, respectively. Experimental runs were generated and ran in random sequence to determine the actual removal efficiency response values from the collected experimental data, while the predicted response values were determined using the quadratic polynomial model as given in Eq. (4):

$$\begin{aligned} Removal\% = {} & +84.09 - 3.59A + 8.35B - 1.59C + 7.65D + 0.1841AB \\ & - 2.16AC + 1.72AD - 2.85BC - 8.24BD - 0.1004CD - 7.25A^2 \\ & + 3.79B^2 - 2.95C^2 - 2.01D^2 \end{aligned} \quad (4)$$

3.4.1. ANOVA for quadratic model

The analysis of variance (ANOVA) was employed to support the acceptability of the design model. Table 3 shows the obtained ANOVA data from the Design-Expert software. According to the results presented, the F-value of the model was 20.66, implying that the model is significant, and there is only a 0.17% chance that an F-value this large could occur due to noise. The significance of the studied model was also confirmed by the very low P-value of the model (P model = 0.0017). This value also relates to describe the close agreement between actual and predicted responses observed in Table 2 [60,61]. The P-value for the linear and quadratic terms of the model was also studied. In this case, the model terms B, D, AD, BC, BD, A^2, and B^2 are significant, showing that solution pH (B), adsorbent dosage (D), and quadratic terms are highly significant, while the other linear and quadratic terms of the model showed low significance.

The Lack of Fit value of 2.85 implies not significant, which is good because we want the model to fit. There is a 20.23% chance that a Lack of Fit F-value this large could occur due to noise. The determination coefficient (R^2) had a value of 0.983, implying that 98% of the variations in this model were predicted and calculated using the established quadratic model. In addition, the calculated adjusted R^2 value (0.935) was close to the predicted R^2 value (0.845) with a difference of less than 0.20. Considering the three R^2 values were high, this indicates that the polynomial model is validated and well fitted to the experimental design responses [51]. The adequacy of the model was further confirmed and validated by the correlation plot between the predicted and actual responses, as shown in Fig. 5a. Moreover, the observed residuals verse the fitted predicted responses were also plotted in Fig. 5b and displayed a normal random distribution of residuals [62].

3.5. Optimization validation

The optimized operating factors suggested by the Design-Expert software were determined as follows; solution pH 7.0 (considering that wastewater or river water is in the range of pH 6–8), initial EE2 hormone concentration 0.30 mg/L, adsorbent dosage 20 mg, and temperature 40 ℃. To optimize the operating parameters, the lower and upper limits of the operating parameters were chosen based on the studied ranges. The target was selected based on the most desirable conditions. The deduced predicted values for removal percentage and adsorption capacity are provided in Table 4. To confirm the generated predicted values, a validation test was performed using the determined optimum conditions. Results showed a close correlation between the predicted and experimental responses, validating the significance of the model.

3.6. Effect of two interaction parameters on the removal of EE2 hormone

The 3D response surface plots help in the comprehensive evaluation of the operation of the system under the framed experimental design and elaborate to understand the effects caused on the response by variation of the experimental factors. The observation obtained are discussed as follows:

Fig. 6a demonstrates the effect of temperature and solution pH on the removal percentage of EE2. As can be seen, an increase and then decrease in removal percentage was observed with an increase in temperature ranging from 25 to 55 ℃. Whereas, a linear rise in removal percentage was seen with an increase in pH because EE2 remains undissociated in this pH range till pH reaches its value of pK_a (10.50) [63,64]. The highest removal percentage recorded was 95.60% at 40 ℃ temperature and pH 9. On the other hand, the lowest removal percentage occurred at pH 5 and a temperature of 55 ℃. This is because the adsorption here is of exothermic nature and spontaneous, which favors lower temperatures [65]. In Fig. 6b, the effect on EE2 removal percentage is observed by varying temperature and concentration of the hormone solution. The EE2 removal percentage increased and then decreased with an increase in temperature, which indicates that the adsorption of EE2 on PU-PANI-ES is exothermic, favoring high removal efficiency at a lower temperature [66]. At a high concentration of hormone 0.4 mg/L and temperature 55 ℃, the removal percentage appears to be the least. The highest removal percentage of 82.10% is found to be at optimum parameters of 40 ℃ and 0.3 mg/L concentration of the hormone. Fig. 6c depicts the effect of temperature and dosage of adsorbent on the removal percentage of EE2. The temperature ranged from 25 to 55 ℃, and the dosage of the adsorbent from 10 to 30 mg. An increase in removal efficiency followed by a decrease with increasing temperature, as described above, relates to the exothermic nature of the adsorption process. However, the removal percentage increased linearly with an increase in the dosage of the adsorbent. This could be due to the increase in the number of sites leading to an increase in the contact surface area as the amount of adsorbent increased [67]. The highest removal percentage achieved was nearly 90%, with a 30 mg dosage of the adsorbent at 40 ℃.

In Fig. 6d, the effect of changing solution pH and concentration of the hormone is seen on the removal percentage. The solution pH ranges from 5 to 9 and concentration from 0.20 to 0.40 mg/L. The removal percentage is slightly high at pH 5 and at a higher concentration of 0.4 mg/L. However, there is a sharp rise in removal percentage from nearly 70.00% at pH 5–96.00% at pH 9. The highest removal percentage is found to be at 0.20 mg/L concentration and pH 9. However, the

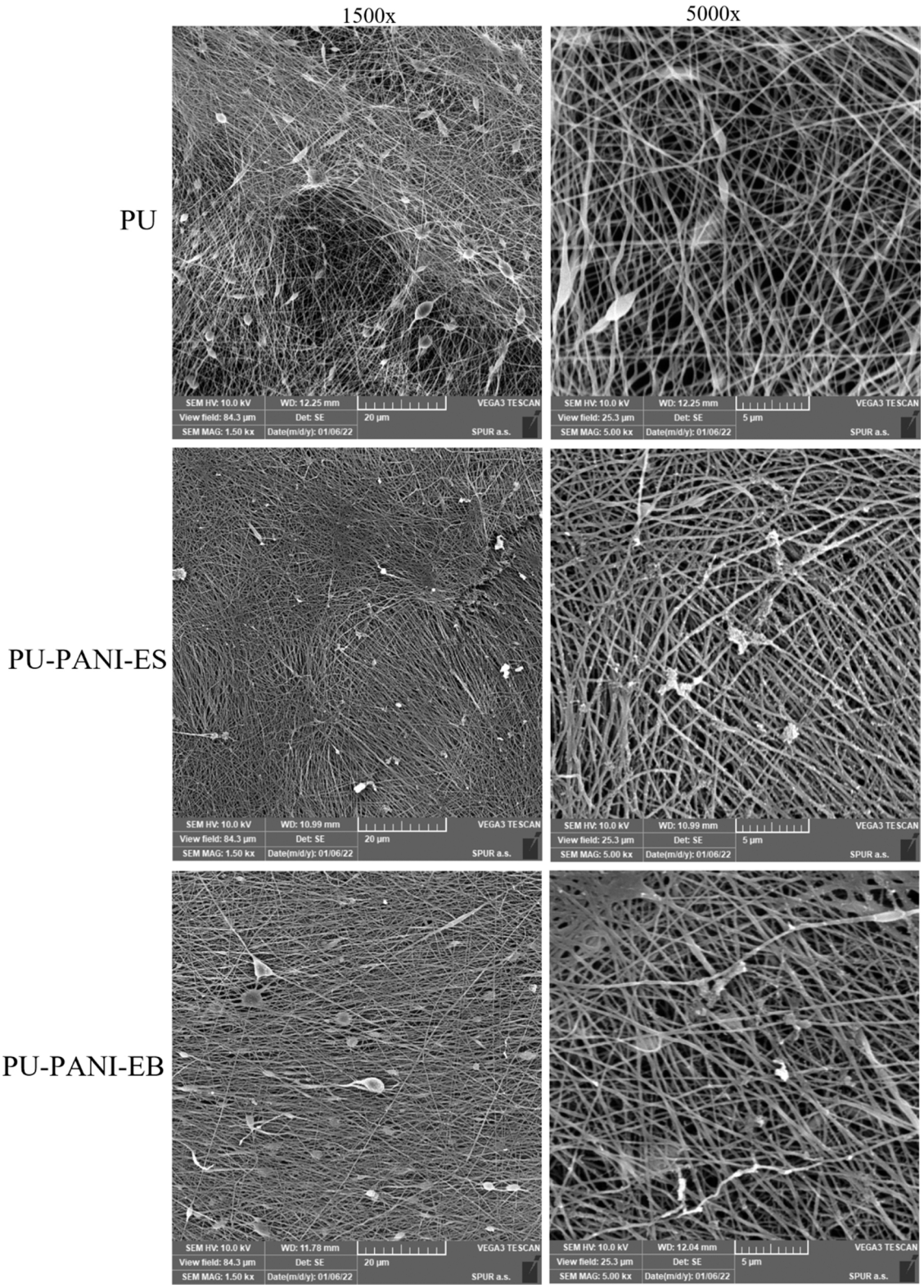

Fig. 3. SEM images of PU as control, PU-PANI-ES, and PU-PANI-EB treated fibers at different magnifications of 1500x and 5000x.

removal percentage is seen to decrease by an increase in concentration from 0.20 to 0.40 mg/L at constant pH 9. A plausible reason could be that all the active sites are already occupied, reaching saturation, and a rise in concentration led to a drop in removal percentage [67]. Fig. 6e illustrates the effect of dosage of adsorbent and solution pH on the removal percentage of EE2. It is evident from the graph that at pH 5 and 10 mg of dosage, the least removal percentage was achieved. Furthermore, the removal percentage linearly increased by either solely an increase in pH of the solution or an increase in the dosage of adsorbent. Whereas, at pH 9, increasing the dosage of adsorbent had a negligible effect on removal percentage, but at pH 5, the difference was distinguishing; a rise in removal percentage from 50.00% at a dosage of

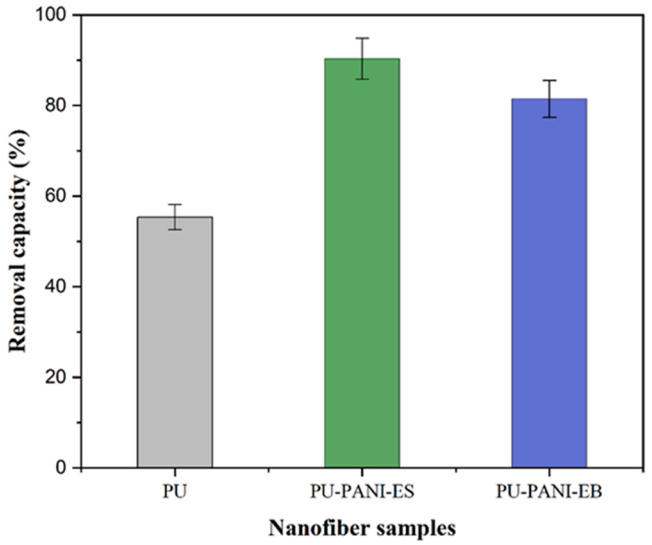

Fig. 4. Adsorption removal of EE2 using PU as control, PU-PANI-ES, and PU-PANI-EB treated nanofibrous membranes.

Table 2
The different experiment runs with their actual and predicted responses.

Runs	Factors				Removal capacity (%)	
	A	*B*	*C*	*D*	*Actual response*	*Predicted response*
1	40	7	0.2	20	84.58	82.72
2	40	7	0.3	20	82.12	84.09
3	40	7	0.3	40	89.17	89.72
4	40	7	0.3	30	85.85	84.09
5	55	9	0.2	10	85.52	85.98
6	40	5	0.3	20	78.98	79.53
7	25	9	0.4	30	83.46	82.72
8	40	9	0.3	20	95.67	96.23
9	55	7	0.3	20	72.70	73.25
11	55	9	0.4	10	85.85	84.09
13	55	5	0.4	30	73.72	72.98
14	40	7	0.3	10	85.85	84.09
15	55	5	0.2	30	80.90	80.16
16	25	5	0.2	10	73.88	74.43
17	25	7	0.3	20	81.68	82.15
18	40	7	0.4	20	52.93	53.39
19	25	5	0.4	10	79.87	80.42
20	25	9	0.2	30	76.59	79.55

10 mg to around 92.00% at a dosage of 30 mg was seen which indicates a rapid rise in adsorption. The highest removal percentage of about 96.00% interpreted from this graph was at pH 9 and 20 mg of dosage. Fig. 6f represents the influence of the concentration of hormone and the dosage of adsorbent on EE2 removal percentage. As can be seen, at a dosage of 10 mg, the removal percentage is the least and is almost unaffected by an increase in the concentration of the solution. However, the removal percentage is high at a lower concentration if the dosage is kept constant. Whereas, there is a gradual rise in the removal percentage by increased dosage of adsorbent for all the given concentrations of the solution. At a dosage of 30 mg, a slight increase and then decrease is observed in the removal percentage of EE2 by the increase in the concentration of the solution. This indicates that the rise was due to an increase in the amount of EE2 hormones adsorbed on the sites of the adsorbent until the 0.30 mg/L concentration of the solution. At this point, all the available sites on the adsorbent were completely filled by EE2 hormones, and a further increase in concentration led to a decrease in removal percentage because no additional EE2 hormone molecule could be adsorbed on the adsorbent's surface [63].

Table 3
ANOVA data for removal of estrogenic hormone based on CCD quadratic model.

Source	Sum of Squares	df	F-value	p-value	
Model	1752.04	14	20.66	0.0017	significant
A-Temperature	25.72	1	4.24	0.094	
B-pH	139.43	1	23.01	0.004	
C-Conc of hormone	25.13	1	4.15	0.097	
D-Dosage of adsorbent	116.93	1	19.30	0.007	
AB	0.05	1	0.09	0.093	
AC	37.39	1	6.17	0.056	
AD	4.76	1	7.85	0.042	
BC	65.17	1	10.76	0.022	
BD	108.62	1	17.93	0.008	
CD	0.08	1	0.01	0.913	
A^2	133.88	1	22.10	0.005	
B^2	36.58	1	6.04	0.006	
C^2	22.18	1	3.66	0.114	
D^2	10.29	1	1.70	0.249	
Residual	30.29	5			
Lack of Fit	19.85	2	2.85	0.202	not significant
Pure Error	10.44	3			
Cor Total	1982.33	19			

3.7. Effect of single parameters on the optimal removal of EE2 hormone

In order to further validate the determined optimum conditions for the removal of EE2 hormone, the removal efficiency and adsorption capacity of PU-PANI-ES adsorbent was evaluated by varying a single factor (solution pH, initial EE2 concentration, dosage, and temperature) while keeping the other factors constant at determining optimum values.

3.7.1. Effect of solution pH

In Fig. 7a, an increasing trend is observed with an increase in the pH of the solution. There is a gentle rise in efficiency from 79.90% at pH 5 to about 82.10% at pH 7; however, there is a sharp increase in efficiency, reaching 95.70% at pH 9. A similar trend was followed for the values of adsorption capacities which were about 1.67, 1.70, and 2.00 mg/g for pH 5, 7, and 9, respectively. Usually, pK_a represents the acid dissociation constant at which EE2 can lose its hydrogen atom and become negatively charged. The pK_a of EE2 is in the range of 10.25–10.50; therefore, in this case, the pH of the solutions remained below 9.5. Thus, no cation-anionic attraction was expected to occur between EE2 and adsorbent, and EE2 remained neutral [68]. However, at higher pH above pK_a, adsorption efficiency is expected to decrease due to charge repulsion [69].

3.7.2. Effect of initial EE2 hormone concentration

Fig. 7b represents the influence of the initial concentration of EE2 in the solution on the efficiency of PU-PANI-ES fibers. It can clearly be seen that the efficiency of fibers linearly decreased, whereas the adsorption capacity increased with an increase in the concentration of EE2 in the solution. At 0.20 mg/L concentration, the highest removal efficiency of 84.62% and lowest adsorption capacity of 1.09 mg/g was reported, while at 0.40 mg/L concentration, the lowest removal efficiency of 76.64% and highest adsorption capacity of 2.21 mg/g was reported. This is because high removal efficiency is expected with a large number of active sites available for adsorption. However, at a higher initial concentration of the solution, less number of sites are left gradually due to saturation leading to a reduction in removal efficiency [67].

3.7.3. Effect of dosage

In Fig. 7c, the effect of adsorbent dosage was determined on its removal efficiency and adsorption capacity. The removal efficiency linearly increased from 73.90% at a dosage of 10 mg to 89.20% at a 40 mg of fiber dosage. The response for adsorption capacity was the

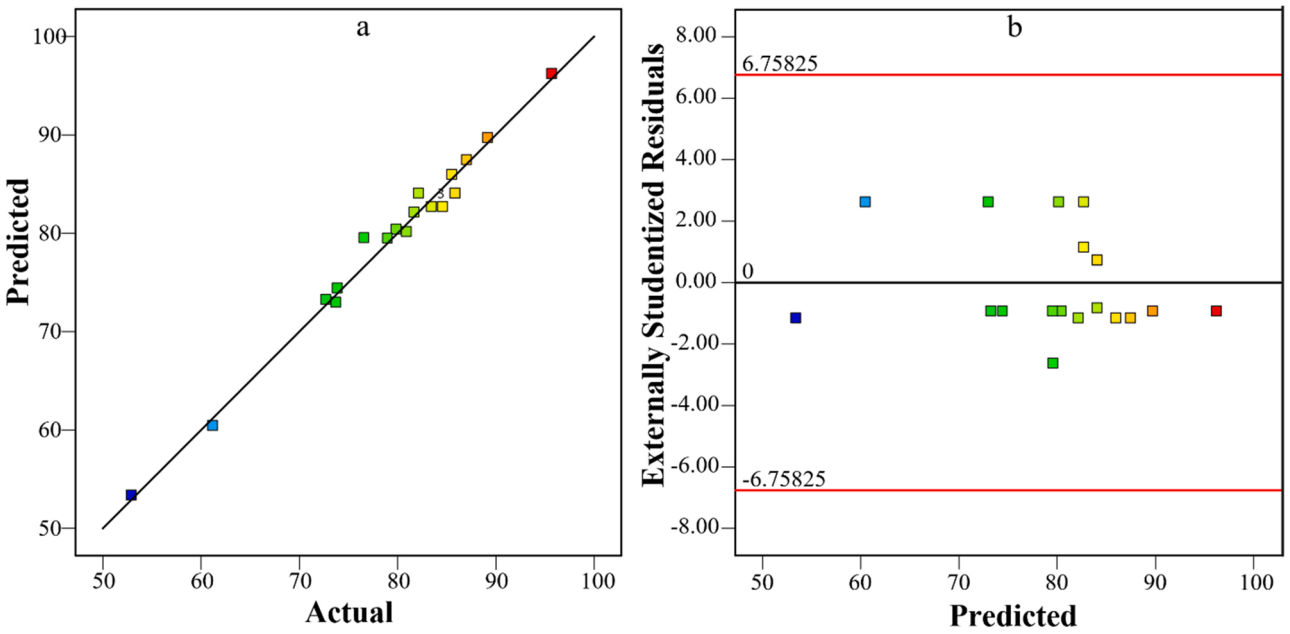

Fig. 5. (a) Plot of predicted and actual responses values and (b) residual plot for EE2 hormone removal.

Table 4
Point prediction and validation of optimized parameters at 95% confidence interval.

Response	Predicted Mean	Observed	Std Dev	SE Mean	Desirability
Removal percentage (%)	84.08	82.20	2.46	0.85	1.00
Adsorption capacity (mg/g)	1.88	2.11	0.29	0.10	1.00

opposite. It was 3.04 mg/g observed at 10 mg of dosage, which decreased to 0.91 mg/g for 40 mg of dosage. This is expected to happen due to the large surface area available at high dosage, creating more number of sites for adsorption. Thus, high removal percentage is observed [63,67].

3.7.4. *Effect of temperature*

In Fig. 7d, the effect of temperature variation was observed on the performance of the coated PU membrane. It can be seen that both removal efficiency and adsorption capacity of coated PU increased between 25 and 35 °C, and then they decreased with further increase in temperature to 55 °C. The optimum temperature observed was 35 °C, with a removal efficiency of 82.10%, and an adsorption capacity of 1.70 mg/g was recorded. The values at a higher temperature of 55 °C were 72.70% and 1.58 mg/g, respectively, which were lower than the values obtained at room temperature of 79.90% and 1.63 mg/g, respectively. This is because the nature of adsorption is exothermic in this case which favors higher adsorption as lower temperature [66]. A more detailed description is given in the later section about thermodynamics.

3.8. *Adsorption mechanism*

The aim of this section is to elucidate the types of mechanisms that occur simultaneously and contribute to the adsorption of EE2 on PU-PANI-ES, as presented in Scheme 3. The extent of such mechanisms depends on the types of functional groups present on the fiber, the nature of the hormone (hydrophobicity), and the amount of surface available on fibers for interaction. Based on the studied material, the types of adsorption interaction mechanisms include physical adsorption, hydrophobic interaction, π–π stacking interaction, cation-π interaction, and hydrogen bonding. EE2 has an OH terminal group, which can act as a strong donor and acceptor, while the benzene ring chain can act as a weak π acceptor [69]. In addition, the presence of high amounts of nitrogen atoms from PU and PANI increases the interaction of the adsorbent with the hormone via a hydrogen bond, electrostatic interaction, and weak van der Waals forces. Furthermore, the physical adsorption of EE2 on the surface of PU-PANI-ES with an approximate average diameter (174 ± 56 nm) and inner pores (16.99 nm) present on the fiber's surface possess a large surface area that contains active sites for accumulation of EE2 hormones [46].

K_{ow} is the parameter value to determine the hydrophobicity of estrogenic hormone by partitioning between octanol and water. Hormones with a value greater than 2.50 are generally expected to accumulate in the solid phase instead of dissolving in an aqueous solution. The K_{ow} of EE2 is 3.67, which is above 2.50; thus, it is likely to undergo hydrophobic interaction with PU. Weak π–π stacking interaction also occurs between the electron-rich and deficient benzene aromatic rings (phenol group) available in PU, PANI, and EE2 hormone by overlapping of double bonds [69]. Comparing the results in Fig. 4, the decrease in adsorption percentage from 90.30% for PU-PANI-ES to 81.50% for PU-PANI-EB is a consequence of the loss of positively charged amine groups in PU-PANI-ES when deprotonated to PU-PANI-EB, which in tend decreases the forms cation-π interaction with the aromatic benzene rings of EE2 [69]. PU is the most robust adsorbing polymer tested among other polymers in the previous study, owing to its polar nature [46]. PU consists of N-H and C═O functional groups that can form hydrogen bonding with the O-H terminal groups present in EE2 [70]. Herein, PU-PANI-ES fibers were chemically functionalised with an excess of amine groups present on the surface, as a result, enhanced the adsorption of EE2 on its surface as compared to the non-coated PU (as control). Furthermore, size-exclusion is another factor essential for membrane filtration, but it is unexpected here in the adsorption mechanism, which is primarily dependent on the molecule size of EE2, the pore size of fibers, and functional properties. The molecular size of hormones reported in the literature (0.79 nm) is far less than the mean porosity of the control PU fibers structure (0.47 μm); hence this factor is excluded from consideration [46,71].

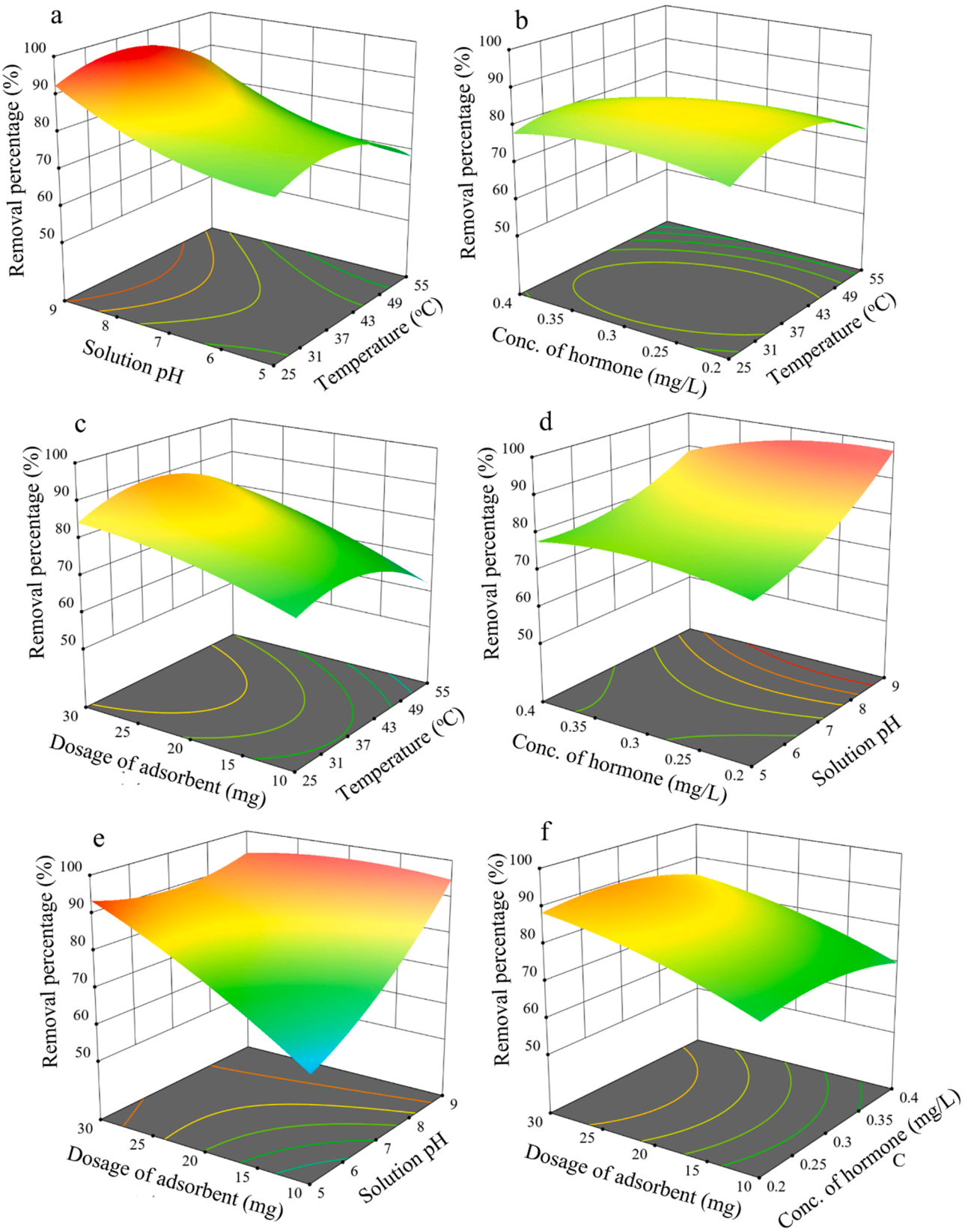

Fig. 6. 3D two parameter interaction response surface plot on the removal of EE2 hormone using PU-PANI-ES membrane.

3.9. Kinetic modelling

To better understand the effects posed on adsorption interactions and determination of the rate-limiting step, kinetic studies on the adsorption process of the hormone was studied. In general, the evaluation of different kinetic models helps in the precise selection of best suited parameters for the optimum removal rates [72]. This is because several mechanisms occur together in a complex closed system which may cause

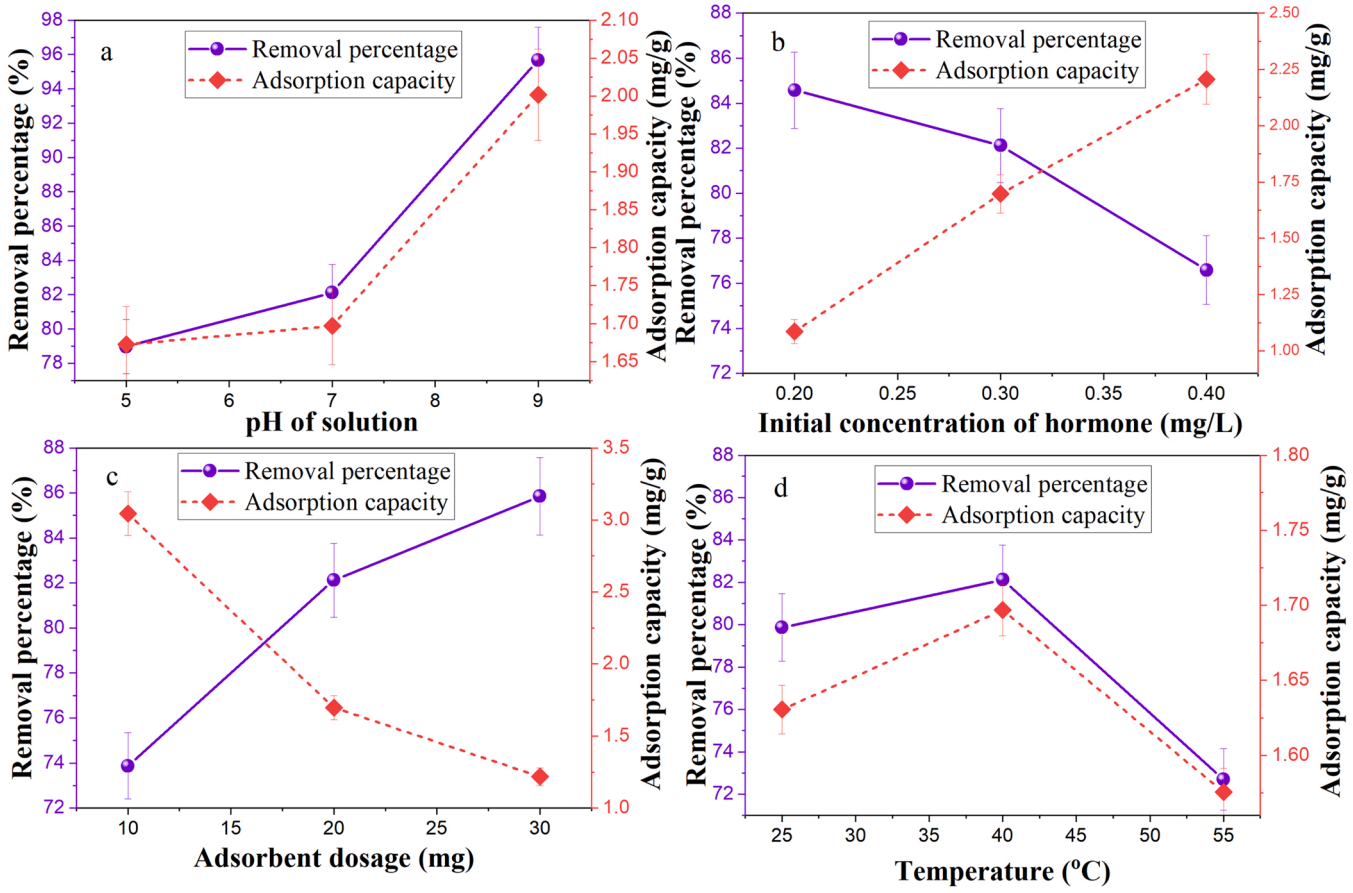

Fig. 7. Effects of different adsorption parameters on removal percentage and adsorption capacity: a) pH of the solution, b) initial concentration of EE2, c) adsorbent dosage, and d) temperature on the removal of EE2 hormone using PU-PANI-ES fibers.

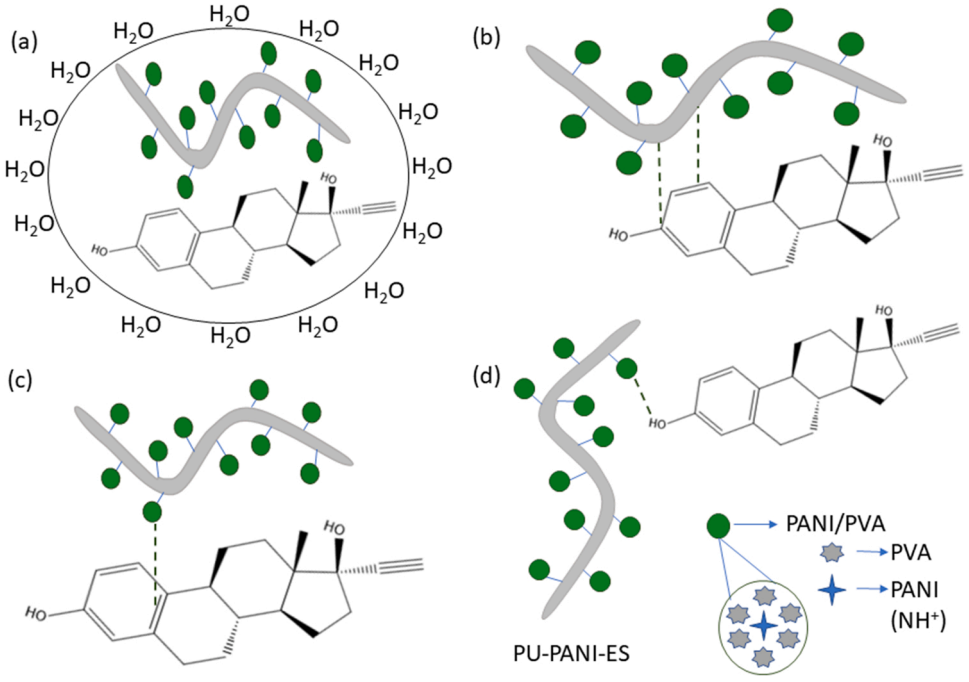

Scheme 3. Possible interaction mechanisms between EE2 and PU-PANI-ES fibers; (a) hydrophobic interactions, (b) π–π stacking interaction, (c) Cation-π interaction, and (d) hydrogen bonding.

surface effects to overshadow the chemical effects during adsorption analysis. Thus, four of the most renowned kinetic models, pseudo-first-order, pseudo-second-order, Weber-Morris intraparticle diffusion, and Boyd's model, were employed for the data generated from the set of experimental values [53,64]. Pseudo-first order model is widely used for explaining the solid/liquids systems to evaluate the adsorption of an adsorbent in an aqueous medium. This model prescribes that the adsorption rate of EE2 hormone is directly proportional to the amount adsorbed from the given aqueous solution. The pseudo-second-order equation predicts the adsorption capacity of the adsorbent over the long-range experimental time. It assumes that the rate-determining step is caused by surface adsorption, which is guided by the physicochemical interactions owing to chemisorption between adsorbent-adsorbate phases. The Weber-Morris intraparticle model to obtain adsorption rates is related to the diffusion of adsorbate towards the adsorbent. This is proportionally dependent on its speed for diffusion. Boyd's model accounts for the free diffusion of a solid spherical adsorbent in a solution phase. The following equations of the stated models are given below, respectively.

$$\log(q_e - q_t) = \log q_e - \frac{K_1}{2.303} t \quad (5)$$

$$\frac{t}{q_t} = \frac{1}{K_2 q_e^2} + \frac{t}{q_e} \quad (6)$$

$$q_t = K_3 t^{0.5} + C \quad (7)$$

$$B_t = -0.4977 - \ln(1 - F) \quad (8)$$

where qe and qt (mg/g) represent the adsorption capacities at equilibrium and time, t, respectively. K_1 (min^{-1}) is the pseudo-1st order adsorption rate constant, K_2 (g/mg min) is the rate constant of the pseudo-2nd order adsorption process. Following the Pseudo-1st order equation, a plot of $log\ (q_e\text{-}q_t)$ versus t (Fig. 8a) was deduced, and the values of K_1 and qe were obtained from the slope and intercept, respectively. A graph of t/q_t versus t (Fig. 8b) was also plotted based on the pseudo-2nd order model to determine the values of K_2 and q_e from the slope and intercept, respectively. K_3 (mg/g $min^{0.5}$) is the intraparticle diffusion rate constant, C (mg/g) is the boundary layer effect that contributes to the rate-limiting adsorption step, Bt is the Boyd parameter related to the adsorption process, and F is the fraction of solute adsorbed at any time, t (min), estimated from $F = q_t/q_{max}$.

Comparing Fig. 8a and b, the difference between the dotted data set experimental points are far away scattered from the line of best fit (Fig. 8a), which indicates that the model was not completely suitable to describe the adsorption interaction between EE2 hormone and PU-PANI-ES adsorbent. Whereas Fig. 8b showed the best fitting with the experimental data indicating the pseudo-second-order model best descript the adsorption process. This is also evident by high regression coefficients and close agreement between the experimental adsorption capacities and the calculated values, represented in Table 5. Fig. 8c and d describe the kind of adsorption process occurring during the uptake of EE2 hormone by PU-PANI-ES. From Fig. 8c, two linear regions are visible (initial half and latter half), which relates to the initial and gradual adsorption

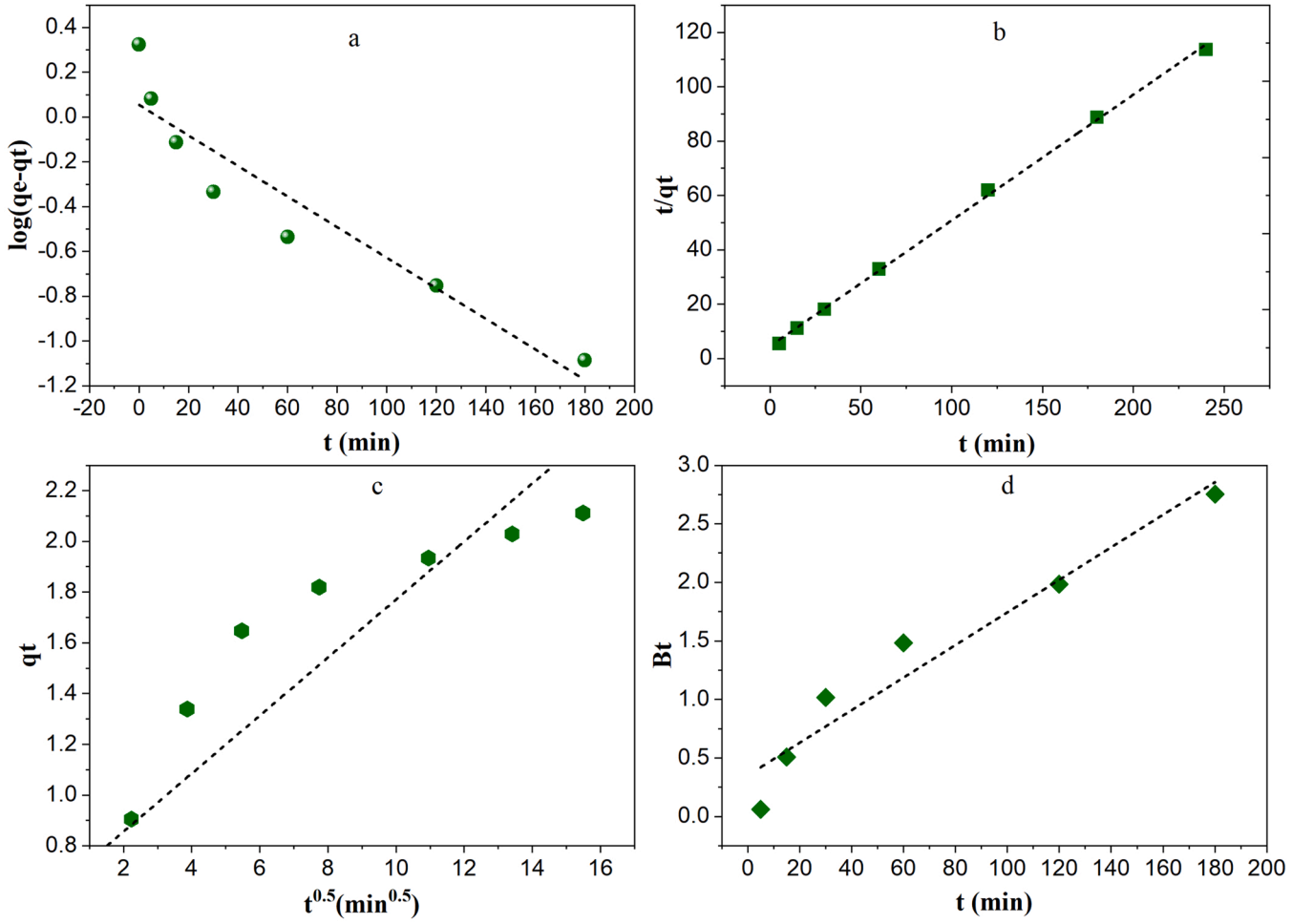

Fig. 8. Plots of the adsorption kinetics for the EE2 hormone on PU-PANI-ES fibers: (a) pseudo-first-order, (b) pseudo-second-order, (c) intraparticle diffusion model, and (d) Boyd model.

Table 5
Kinetic models and their determining parameters related to the removal of EE2 hormone using PU-PANI-ES fibers.

Pseudo-first-order		**Pseudo-second order**	
$q_{e,}$ *exp (mg/g)*	2.11	$q_{e,}$ *exp (mg/g)*	2.11
$q_{e,}$ *cal (mg/g)*	1.13	$q_{e,}$ *cal (mg/g)*	2.16
K_1 *(min^{-1})*	0.02	K_2 *(g/mg min)*	0.04
R^2	0.892	R^2	0.998
χ^2	0.03	χ^2	0.12
SSE	0.16	*SSE*	0.57
Intraparticle diffusion		**Boyd**	
K_3 *(mg/g min$^{0.5}$)*	0.11	R^2	0.939
C (mg/g)	0.62	χ^2	0.07
R^2	0.872	*SSE*	0.29
χ^2	0.14		
SSE	0.84		

phase and then the equilibrium phase. In addition, the boundary-layer effect was depicted not to pass through the origin region, which indicates that the process was more intraparticle diffusion-controlled in the latter half of the experiment as a consequence of the surface control effect [64,65].

Among all the calculated models from the experimental data, it can be seen that EE2 adsorption on PU-PANI-ES fibers follows the pseudo-second-order model. The experimental data set points adhere completely to the line of best fit, also observed by the high regression coefficient (R^2) of 0.998 and the calculated adsorption capacity of 2.16 mg/g is extremely close to the experimental value of 2.11 mg/g. The plausible reason that indicates these findings could be the inhomogeneous surface of available active sites on the modified adsorbent PU membrane since the adsorption rate is dependent on the concentration of hormone in the solution and the number of available sites that can actively accommodate the hormone [73]. All the supporting values of the given models are presented in Table 5.

3.10. Thermodynamic study

In order to understand the thermodynamic behavior of the adsorption process for the removal of EE2 by PU-PANI-ES adsorbent, the Gibbs free energy change (ΔG), enthalpy change (ΔH), and entropy change (ΔS) were determined using Eqs. (9)–(11) [74,75]. The thermodynamic parameters were calculated based on the adsorption distribution coefficient (K_D) for the different studied temperatures.

$$K_D = \frac{C_s}{C_e} \tag{9}$$

$$lnK_D = -\frac{\Delta H}{RT} + \frac{\Delta S}{R} \tag{10}$$

$$\Delta G = \Delta H - T\Delta S \tag{11}$$

where K_D is the distribution coefficient (a ratio of solid phase to solute concentrations), R (8.314 J/mol K) is the universal gas constant, C_s (mg/L) is the concentration of EE2 on the adsorbent, and T (K) is the absolute temperature. By plotting a Van't Hoff plot of lnK_D versus $1/T$, ΔS and ΔH were determined from the slope and intercept, respectively. Values of ΔG at different temperatures were then calculated and are given in Table 6.

Table 6
Thermodynamic parametric values for the adsorption of EE2 hormone.

Parameters	Temperature		
	298 K	*313 K*	*328 K*
ΔG (kJ/mol)	-37.52	-33.03	-28.53
ΔH (kJ/mol)	-12.67		
ΔS (J/mol K)	-29.94		

In accordance with calculated results, ΔG was determined to be negative, which is expected, indicating that the adsorption process was favourable and the reaction was spontaneous. ΔH value was negative, which confirmed the adsorption of EE2 onto the PU-PANI-ES membrane to be exothermic in nature. This explains the decrease in adsorption capacity at higher temperatures. In addition, the low ΔH value depicts the adsorption process favour more physical adsorption rather than chemical adsorption. The values deduced and phenomena observed in the present study are in close agreement with similar previous studies on the adsorption of estrogenic hormones [64,76]. The negative ΔS value indicates the adsorption process was more enthalpy driven.

3.11. Reusability study

It could be noticed from the results in Fig. 9 that the adsorption efficiency of PU-PANI-ES for EE2 hormone remains over 80% throughout the six adsorption cycles, while desorption gradually decreases and stay stagnant at around 60% in the last two cycles. A slight rise in adsorption with the increase in the number of cycles up to four cycles was observed, which could be due to improved swelling of the adsorbent when in contact with the ethanol (alkaline medium), resulting in high adsorption. However, the efficiency gets constant and near to that of the first cycle during the fifth and sixth cycles, which can be attributed to the decrease in the swelling reversibility of PU-PANI-ES. A similar increasing and then decreasing trend was reported in the literature for acid orange II and methylene blue removal [77].

3.12. Comparative study with other adsorbents

The following Table 7 demonstrates the adsorbent fibers and particles reported in the literature with their total adsorption capacities for capturing EE2 hormone compared to this study. As can be seen, the adsorption capacity of PU-PANI-ES reported in this study is 2.11 mg/g. This value is relatively high compared to similar reported previous studies. It is noteworthy to mention the significance of produced electrospun modified nanofibrous membrane in this study. However, considering Norit AC, Darco AC, and PA612 particles, the adsorption capacity value of these materials is still quite higher than the current study, which can be attributed to the nature of those materials and the relatively large surface area they possess (5.12–17.64 m^2/g) in general as compared to fibrous materials.

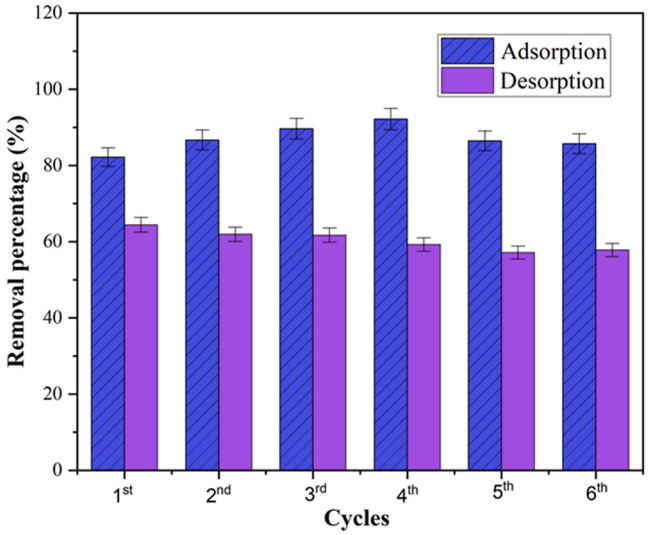

Fig. 9. Six adsorption-desorption cycles of EE2 by PU-PANI-ES fibers.

Table 7
Comparison of adsorbents for EE2 hormone removal.

Adsorbents	pH and temperature (°C)	Adsorption capacity (mg/g)	Reference
MWCNTs	6.30 and 25	0.47	[64]
PA612, Darco AC, Norit AC	7.00 and 25	25.42 27.61 10.40	[78]
Un-anthracite, 4 K anthracite	7.00 and 25	0.21 0.62	[79]
PU Elastollan, PU 918, PA	7.00 and 25	0.74 0.64 0.61	Our previous work [46]
PU-PANI-ES	7.00 and 40	2.11	**Present study**

4. Conclusions

In this study, we successfully investigated the removal of a steroid hormone from water by lab synthesized spun polyurethane nanofiber membrane modified with PANI in PVA solution as the supporting polymer. The different spun and treated PU nanofiber membranes were chemically and morphologically characterized via FTIR, SEM, and optical microscopy. PU-PANI-ES as a modified material demonstrated to be the most efficient with 90.30% removal efficiency of the studied hormone as compared to its base form PU-PANI-EB (81.50%) and neat PU (55.40%) as control. PU-PANI-ES was further evaluated via an optimization study using the CCD model to determine its optimum removal conditions for EE2 hormone. According to the results obtained, the model proved to be significant for the optimization of the removal of the EE2 hormone with a high regression coefficient (R^2) of 0.983. The optimum parameters were found to be pH 7 (considering that wastewater or river water is in the range of pH 6–8), the temperature of 40 °C, 0.3 mg/L concentration of EE2, and 20 mg of PU-PANI-ES dosage. In addition, the adsorption was studied kinetically using different kinetic models, and the results depicted that the removal of EE2 hormone best fitted the pseudo-second-order model with maximum adsorption capacity determined as 2.11 mg/g. This obtained value proved to be significantly high compared to the other similar adsorbents in the literature. Furthermore, the adsorption efficiency was demonstrated to be temperature sensitive and decreased considerably at a higher temperature. This was supported by a thermodynamic study that showed the adsorption process is spontaneous and exothermic in nature. Finally, the recovery of EE2 hormone and reusability of PU-PANI-ES adsorbent depicted a good removal percentage which remained over 80% for tested six consecutive adsorption-desorption cycles. Overall, the reported results proved that the modification of the spun PU nanofiber with PANI significantly improved hormone removal from water and can be considered a promising adsorbent membrane for the remediation of different steroid hormones from water.

CrediT authorship contribution statement

Muhammad Yasir: Conceptualization, Methodology, Investigation, Formal analysis, Data curation, Writing – original draft, Writing – review & editing. **Fahanwi Asabuwa Ngwabebhoh:** Formal analysis, Data curation, Writing – review & editing. **Tomáš Šopík:** Methodology, Formal analysis, Data curation. **Hassan Ali:** Writing – review & editing. **Vladimír Sedlařík:** Conceptualization, Supervision, Project administration, Funding acquisition, Writing – review & editing.

Declaration of Competing Interest

The authors declare that they have no known competing financial interests or personal relationships that could have appeared to influence the work reported in this paper.

Acknowledgements

The authors gratefully acknowledge the financial support from the Ministry of Education, Youth and Sports of Czech Republic (DKRVO RP/CPS/2022/002 and RP/CPS/2022/005), the Internal Grant Agency of TBU in Zlin (grant no. IGA/CPS/2022/003). We would also like to acknowledge the Centre of Polymer Systems (CPS) situated at Tomas Bata University in Zlin, Czech Republic, to use the available research facilities to conduct this research work.

References

[1] D.V. Henley, J. Lindzey, K.S. Korach, Steroid hormones, in: S. Melmed, P.M. Conn (Eds.), Endocrinology, Humana Press, Totowa, NJ, 2005, pp. 49–65, https://doi.org/10.1007/978-1-59259-829-8_4.
[2] S.M. Choi, S.D. Yoo, B.M. Lee, Toxicological characteristics of endocrine-disrupting chemicals: developmental toxicity, carcinogenicity, and mutagenicity, J. Toxicol. Environ. Health Part B (2004), https://doi.org/10.1080/716100635.
[3] M.E. Street, S. Angelini, S. Bernasconi, E. Burgio, A. Cassio, C. Catellani, F. Cirillo, A. Deodati, E. Fabbrizi, V. Fanos, G. Gargano, E. Grossi, L. Iughetti, P. Lazzeroni, A. Mantovani, L. Migliore, P. Palanza, G. Panzica, A.M. Papini, S. Parmigiani, B. Predieri, C. Sartori, G. Tridenti, S. Amarri, Current knowledge on endocrine disrupting chemicals (EDCs) from animal biology to humans, from pregnancy to adulthood: highlights from a national italian meeting, Int. J. Mol. Sci. (2018), https://doi.org/10.3390/ijms19061647.
[4] M.A. La Merrill, L.N. Vandenberg, M.T. Smith, W. Goodson, P. Browne, H. B. Patisaul, K.Z. Guyton, A. Kortenkamp, V.J. Cogliano, T.J. Woodruff, L. Rieswijk, H. Sone, K.S. Korach, A.C. Gore, L. Zeise, R.T. Zoeller, Consensus on the key characteristics of endocrine-disrupting chemicals as a basis for hazard identification, Nat. Rev. Endocrinol. 16 (2020) 45–57, https://doi.org/10.1038/s41574-019-0273-8.
[5] R. Lauretta, A. Sansone, M. Sansone, F. Romanelli, M. Appetecchia, Endocrine disrupting chemicals: effects on endocrine glands, Front. Endocrinol. 10 (2019).
[6] T.T. Schug, A.F. Johnson, L.S. Birnbaum, T. Colborn, L.J. Guillette, D.P. Crews, T. Collins, A.M. Soto, F.S. vom Saal, J.A. McLachlan, C. Sonnenschein, J.J. Heindel, Minireview: endocrine disruptors: past lessons and future directions, Mol. Endocrinol. 30 (2016) 833–847, https://doi.org/10.1210/me.2016-1096.
[7] C.L.S. Vilela, J.P. Bassin, R.S. Peixoto, Water contamination by endocrine disruptors: impacts, microbiological aspects and trends for environmental protection, Environ. Pollut. (2018), https://doi.org/10.1016/j.envpol.2017.12.098.
[8] Directive (EU) 2020/2184 on the quality of water intended for human consumption (recast), 2021.
[9] M.R. Mills, K. Arias-Salazar, A. Baynes, L.Q. Shen, J. Churchley, N. Beresford, C. Gayathri, R.R. Gil, R. Kanda, S. Jobling, T.J. Collins, Removal of ecotoxicity of 17α-ethinylestradiol using TAML/peroxide water treatment, Sci. Rep. (2015), https://doi.org/10.1038/srep10511.
[10] C.L.S. Vilela, H.D.M. Villela, G.A.S. Duarte, E.P. Santoro, C.T.C.C. Rachid, R. S. Peixoto, Estrogen induces shift in abundances of specific groups of the coral microbiome, Sci. Rep. 11 (2021) 2767, https://doi.org/10.1038/s41598-021-82387-x.
[11] X. Gao, S. Kang, R. Xiong, M. Chen, Environment-friendly removal methods for endocrine disrupting chemicals, Sustainability 12 (2020) 7615, https://doi.org/10.3390/su12187615.
[12] Z. Křesinová, L. Linhartová, A. Filipová, M. Ezechiáš, P. Mašín, T. Cajthaml, Biodegradation of endocrine disruptors in urban wastewater using Pleurotus ostreatus bioreactor, New Biotechnol. 43 (2018) 53–61, https://doi.org/10.1016/j.nbt.2017.05.004.
[13] R.M. Castellanos, J.P. Bassin, D.M. Bila, M. Dezotti, Biodegradation of natural and synthetic endocrine-disrupting chemicals by aerobic granular sludge reactor: Evaluating estrogenic activity and estrogens fate, Environ. Pollut. 274 (2021), 116551, https://doi.org/10.1016/j.envpol.2021.116551.
[14] X. Wei, J. Li, Z. Liu, X. Yang, S. Naraginti, X. Xu, X. Wang, Visible light photocatalytic mineralization of 17α-ethinyl estradiol (EE2) and hydrogen evolution over silver and strontium modified TiO 2 nanoparticles: mechanisms and phytotoxicity assessment, RSC Adv. 8 (2018) 4329–4339, https://doi.org/10.1039/C7RA12638G.
[15] R.V. Carvalho, B.G. Isecke, E. Carvalho, F.J.C. Teran, Photocatalytic oxidation of 17 -Ethinylestradiol by UV-activated TiO2 in batch and continuous-flow reactor, J. Chem. Eng. Mater. Sci. (2017), https://doi.org/10.5897/jcems2017.0293.
[16] A. Rafiq, M. Ikram, S. Ali, F. Niaz, M. Khan, Q. Khan, M. Maqbool, Photocatalytic degradation of dyes using semiconductor photocatalysts to clean industrial water pollution, J. Ind. Eng. Chem. 97 (2021) 111–128, https://doi.org/10.1016/j.jiec.2021.02.017.
[17] M. Naz, A. Rafiq, M. Ikram, A. Haider, S.O.A. Ahmad, J. Haider, S. Naz, Elimination of dyes by catalytic reduction in the absence of light: a review, J. Mater. Sci. 56 (2021) 15572–15608, https://doi.org/10.1007/s10853-021-06279-1.
[18] M. Yasir, M. Masar, T. Sopik, H. Ali, M. Urbanek, J. Antos, M. Machovsky, I. Kuritka, ZnO nanowires and nanorods based ZnO/WO3/Pt heterojunction for efficient photocatalytic degradation of Estriol (E3) hormone, Mater. Lett. (2022), 132291, https://doi.org/10.1016/j.matlet.2022.132291.

[19] T.A. Saleh, Carbon nanotube-incorporated alumina as a support for MoNi catalysts for the efficient hydrodesulfurization of thiophenes, Chem. Eng. J. 404 (2021), 126987, https://doi.org/10.1016/j.cej.2020.126987.
[20] T.A. Saleh, Protocols for synthesis of nanomaterials, polymers, and green materials as adsorbents for water treatment technologies, Environ. Technol. Innov. 24 (2021), 101821, https://doi.org/10.1016/j.eti.2021.101821.
[21] K.J. Choi, S.G. Kim, C.W. Kim, S.H. Kim, Effects of activated carbon types and service life on removal of endocrine disrupting chemicals: amitrol, nonylphenol, and bisphenol-A, Chemosphere (2005), https://doi.org/10.1016/j.chemosphere.2004.11.080.
[22] E. Kim, C. Jung, J. Han, N. Her, C. Min Park, A. Son, Y. Yoon, Adsorption of selected micropollutants on powdered activated carbon and biochar in the presence of kaolinite, Desalin. Water Treat. (2016), https://doi.org/10.1080/19443994.2016.1175972.
[23] A.O. Ifelebuegu, Removal of steriod hormones by activated carbon adsorption—kinetic and thermodynamic studies, J. Environ. Prot. (2012), https://doi.org/10.4236/jep.2012.36057.
[24] S.O. Badmus, T.A. Oyehan, T.A. Saleh, Enhanced efficiency of polyamide membranes by incorporating cyclodextrin-graphene oxide for water purification, J. Mol. Liq. 340 (2021), 116991, https://doi.org/10.1016/j.molliq.2021.116991.
[25] A.Q. Al-Gamal, T.A. Saleh, F.I. Alghunaimi, Nanofiltration membrane with high flux and oil rejection using graphene oxide/ β-cyclodextrin for produced water reuse, Mater. Today Commun. 31 (2022), 103438, https://doi.org/10.1016/j.mtcomm.2022.103438.
[26] A.Q. Al-Gamal, W.S. Falath, T.A. Saleh, Enhanced efficiency of polyamide membranes by incorporating TiO2-Graphene oxide for water purification, J. Mol. Liq. 323 (2021), https://doi.org/10.1016/j.molliq.2020.114922.
[27] M.S. Islam, B.C. Ang, A. Andriyana, A.M. Afifi, A review on fabrication of nanofibers via electrospinning and their applications, SN Appl. Sci. 1 (2019) 1248, https://doi.org/10.1007/s42452-019-1288-4.
[28] I. Tlili, T.A. Alkanhal, Nanotechnology for water purification: electrospun nanofibrous membrane in water and wastewater treatment, J. Water Reuse Desalin. (2019), https://doi.org/10.2166/wrd.2019.057.
[29] T.A. Saleh, Nanomaterials: classification, properties, and environmental toxicities, Environ. Technol. Innov. 20 (2020), 101067, https://doi.org/10.1016/j.eti.2020.101067.
[30] F.A. AlAbduljabbar, S. Haider, F.A.A. Ali, A.A. Alghyamah, W.A. Almasry, R. Patel, I.M. Mujtaba, Efficient photocatalytic degradation of organic pollutant in wastewater by electrospun functionally modified polyacrylonitrile nanofibers membrane anchoring TiO2 nanostructured, Membranes 11 (2021) 785, https://doi.org/10.3390/membranes11100785.
[31] A.S.M. Ali, M.R. El-Aassar, F.S. Hashem, N.A. Moussa, Surface modified of cellulose acetate electrospun nanofibers by polyaniline/β-cyclodextrin composite for removal of cationic dye from aqueous medium, Fibers Polym. 20 (2019) 2057–2069, https://doi.org/10.1007/s12221-019-9162-y.
[32] S. Yan, Y. Yu, R. Ma, J. Fang, The formation of ultrafine polyamide 6 nanofiber membranes with needleless electrospinning for air filtration, Polym. Adv. Technol. 30 (2019) 1635–1643, https://doi.org/10.1002/pat.4594.
[33] F.S. Victor, V. Kugarajah, M. Bangaru, S. Ranjan, S. Dharmalingam, Electrospun nanofibers of polyvinylidene fluoride incorporated with titanium nanotubes for purifying air with bacterial contamination, Environ. Sci. Pollut. Res. 28 (2021) 37520–37533, https://doi.org/10.1007/s11356-021-13202-3.
[34] M.H. Mohraz, F. Golbabaei, I.J. Yu, M.A. Mansournia, A.S. Zadeh, S.F. Dehghan, Preparation and optimization of multifunctional electrospun polyurethane/chitosan nanofibers for air pollution control applications, Int. J. Environ. Sci. Technol. 16 (2019) 681–694, https://doi.org/10.1007/s13762-018-1649-3.
[35] R. Sarika, D.R. Shankaran, Synthesis and characterization of curcumin nanoparticles loaded nanofibers for lead ion detection, Sens. Lett. (2016), https://doi.org/10.1166/sl.2016.3707.
[36] S. Patel, M. Konar, H. Sahoo, G. Hota, Surface functionalization of electrospun PAN nanofibers with ZnO-Ag heterostructure nanoparticles: synthesis and antibacterial study, Nanotechnology (2019), https://doi.org/10.1088/1361-6528/ab045d.
[37] M.M. Foumani, A. Khorshidi, A.F. Shojaei, Polyethyleneimine nanofibers functionalized with tetradentate Schiff base complexes of dioxomolybdenum(VI) as efficient catalysts for epoxidation of alkenes, ChemistrySelect (2019), https://doi.org/10.1002/slct.201803047.
[38] B. Balusamy, A. Senthamizhan, T. Uyar, Functionalized electrospun nanofibers as a versatile platform for colorimetric detection of heavy metal ions in water: a review, Materials (2020), https://doi.org/10.3390/ma13102421.
[39] R. Araga, C.S. Sharma, Amine functionalized electrospun cellulose nanofibers for fluoride adsorption from drinking water, J. Polym. Environ. (2019), https://doi.org/10.1007/s10924-019-01394-2.
[40] L. Qian, X. Li, F. Qi, J. Li, L. Lu, Q. Xu, An amino-functionalized grooved nanofiber mat for solid-phase extraction of phenolic pollutants, Microchim. Acta (2017), https://doi.org/10.1007/s00604-017-2313-1.
[41] J. Stejskal, P. Bober, M. Trchová, A. Kovalcik, J. Hodan, J. Hromádková, J. Prokeš, Polyaniline cryogels supported with poly(vinyl alcohol): soft and conducting, Macromolecules (2017), https://doi.org/10.1021/acs.macromol.6b02526.
[42] Z. Zhang, Z. Wei, M. Wan, Nanostructures of polyaniline doped with inorganic acids, Macromolecules (2002), https://doi.org/10.1021/ma020199v.
[43] J. Stejskal, Interaction of conducting polymers, polyaniline and polypyrrole, with organic dyes: polymer morphology control, dye adsorption and photocatalytic decomposition, Chem. Pap. (2020), https://doi.org/10.1007/s11696-019-00982-9.
[44] M. Ayad, G. El-Hefnawy, S. Zaghlol, Facile synthesis of polyaniline nanoparticles; its adsorption behavior, Chem. Eng. J. (2013), https://doi.org/10.1016/j.cej.2012.11.099.
[45] J. Stejskal, Conducting polymers are not just conducting: a perspective for emerging technology, Polym. Int. (2020), https://doi.org/10.1002/pi.5947.
[46] M. Yasir, T. Šopík, L. Lovecká, D. Kimmer, V. Sedlařík, The adsorption, kinetics, and interaction mechanisms of various types of estrogen on electrospun polymeric nanofiber membranes, Nanotechnology 33 (2021) 75702, https://doi.org/10.1088/1361-6528/ac357b.
[47] S. Zaghlol, W.A. Amer, M.H. Shaaban, M.M. Ayad, P. Bober, J. Stejskal, Conducting macroporous polyaniline/poly(vinyl alcohol) aerogels for the removal of chromium(VI) from aqueous media, Chem. Pap. 74 (2020) 3183–3193, https://doi.org/10.1007/s11696-020-01151-z.
[48] P. Humpolicek, V. Kasparkova, P. Saha, J. Stejskal, Biocompatibility of polyaniline, Synth. Met. (2012), https://doi.org/10.1016/j.synthmet.2012.02.024.
[49] A.M. Khalil, A.I. Schäfer, Cross-linked β-cyclodextrin nanofiber composite membrane for steroid hormone micropollutant removal from water, J. Memb. Sci. 618 (2021), 118228, https://doi.org/10.1016/j.memsci.2020.118228.
[50] T. Huang, S. wen Zhang, J. Xie, L. Zhou, L. fei Liu, Effective adsorption of quadrivalent cerium by synthesized laurylsulfonate green rust in a central composite design, J. Environ. Sci. (2021), https://doi.org/10.1016/j.jes.2021.01.028.
[51] F.A. Ngwabebhoh, A. Erdem, U. Yildiz, Synergistic removal of Cu(II) and nitrazine yellow dye using an eco-friendly chitosan-montmorillonite hydrogel: Optimization by response surface methodology, J. Appl. Polym. Sci. 133 (2016) 1–14, https://doi.org/10.1002/app.43664.
[52] J. Wang, H. Chi, A. Zhou, R. Zheng, H. Bai, T. Zhang, Facile synthesis of multi-functional elastic polyaniline/polyvinyl alcohol composite gels by a solution assembly method, RSC Adv. (2020), https://doi.org/10.1039/d0ra02238a.
[53] A. Erdem, F.A. Ngwabebhoh, S. Çetintaş, D. Bingöl, U. Yildiz, Fabrication and characterization of novel macroporous Jeffamine/diamino hexane cryogels for enhanced Cu(II) metal uptake: optimization, isotherms, kinetics and thermodynamic studies, Chem. Eng. Res. Des. (2017), https://doi.org/10.1016/j.cherd.2016.10.010.
[54] T.A. Saleh, Isotherm, kinetic, and thermodynamic studies on Hg(II) adsorption from aqueous solution by silica- multiwall carbon nanotubes, Environ. Sci. Pollut. Res. 22 (2015) 16721–16731, https://doi.org/10.1007/s11356-015-4866-z.
[55] T.A. Saleh, The influence of treatment temperature on the acidity of MWCNT oxidized by HNO 3 or a mixture of HNO 3 /H 2 SO 4, Appl. Surf. Sci. 257 (2011) 7746–7751, https://doi.org/10.1016/j.apsusc.2011.04.020.
[56] T.A. Saleh, Simultaneous adsorptive desulfurization of diesel fuel over bimetallic nanoparticles loaded on activated carbon, J. Clean. Prod. 172 (2018) 2123–2132, https://doi.org/10.1016/j.jclepro.2017.11.208.
[57] A. Bahadur, M. Shoaib, A. Saeed, S. Iqbal, FT-IR spectroscopic and thermal study of waterborne polyurethane-acrylate leather coatings using tartaric acid as an ionomer, E Polym. (2016), https://doi.org/10.1515/epoly-2016-0154.
[58] M. Shahi, A. Moghimi, B. Naderizadeh, B. Maddah, Electrospun PVA-PANI and PVA-PANI-AgNO3 composite nanofibers, Sci. Iran. (2011), https://doi.org/10.1016/j.scient.2011.08.013.
[59] H. Huang, J. Yao, L. Li, F. Zhu, Z. Liu, X. Zeng, X. Yu, Z. Huang, Reinforced polyaniline/polyvinyl alcohol conducting hydrogel from a freezing–thawing method as self-supported electrode for supercapacitors, J. Mater. Sci. (2016), https://doi.org/10.1007/s10853-016-0137-8.
[60] O.F.S. Khasawneh, P. Palaniandy, P. Palaniandy, M. Ahmadipour, H. Mohammadi, M.R. Bin Hamdan, Removal of acetaminophen using Fe2O3-TiO2nanocomposites by photocatalysis under simulated solar irradiation: optimization study, J. Environ. Chem. Eng. (2021), https://doi.org/10.1016/j.jece.2020.104921.
[61] M. Galedari, M. Mehdipour Ghazi, S. Rashid Mirmasoomi, Photocatalytic process for the tetracycline removal under visible light: presenting a degradation model and optimization using response surface methodology (RSM), Chem. Eng. Res. Des. (2019), https://doi.org/10.1016/j.cherd.2019.03.031.
[62] D. Lambropoulou, E. Evgenidou, V. Saliverou, C. Kosma, I. Konstantinou, Degradation of venlafaxine using TiO2/UV process: Kinetic studies, RSM optimization, identification of transformation products and toxicity evaluation, J. Hazard. Mater. (2017), https://doi.org/10.1016/j.jhazmat.2016.04.074.
[63] F. Esmaeeli, S.A. Gorbanian, N. Moazezi, Removal of estradiol valerate and progesterone using powdered and granular activated carbon from aqueous solutions, Int. J. Environ. Res. 11 (2017) 695–705, https://doi.org/10.1007/s41742-017-0060-0.
[64] L.A. Al-Khateeb, A.Y. Obaid, N.A. Asiri, M. Abdel Salam, Adsorption behavior of estrogenic compounds on carbon nanotubes from aqueous solutions: Kinetic and thermodynamic studies, J. Ind. Eng. Chem. 20 (2014) 916–924, https://doi.org/10.1016/j.jiec.2013.06.023.
[65] F.F. Qi, Y. Cao, M. Wang, F. Rong, Q. Xu, Nylon 6 electrospun nanofibers mat as effective sorbent for the removal of estrogens: kinetic and thermodynamic studies, Nanoscale Res. Lett. 9 (2014) 1–10, https://doi.org/10.1186/1556-276X-9-353.
[66] L. Kovalova, D.R.U. Knappe, K. Lehnberg, C. Kazner, J. Hollender, Removal of highly polar micropollutants from wastewater by powdered activated carbon, Environ. Sci. Pollut. Res. (2013), https://doi.org/10.1007/s11356-012-1432-9.
[67] S.A. Abdel-Gawad, H.M. Abdel-Aziz, Removal of ethinylestradiol by adsorption process from aqueous solutions using entrapped activated carbon in alginate biopolymer: isotherm and statistical studies, Appl. Water Sci. 9 (2019) 1–8, https://doi.org/10.1007/s13201-019-0951-7.
[68] L.D. Nghiem, A.I. Schäfer, Adsorption and transport of trace contaminant estrone in NF/RO membranes, Environ. Eng. Sci. 19 (2002) 441–451, https://doi.org/10.1089/109287502320963427.

[69] A.I. Schäfer, I. Akanyeti, A.J.C. Semião, Micropollutant sorption to membrane polymers: a review of mechanisms for estrogens, Adv. Colloid Interface Sci. 164 (2011) 100–117, https://doi.org/10.1016/j.cis.2010.09.006.
[70] M. Yasir, T. Sopik, R. Patwa, D. Kimmer, V. Sedlarik, Adsorption of estrogenic hormones in aqueous solution using electrospun nanofibers from waste cigarette butts: Kinetics, mechanism, and reusability, Express Polym. Lett. 16 (2022) 624–648.
[71] A.I. Schäfer, K. Stelzl, M. Faghih, S. Sen Gupta, K.R. Krishnadas, S. Heißler, T. Pradeep, Poly(ether sulfone) nanofibers impregnated with β-cyclodextrin for increased micropollutant removal from water, ACS Sustain. Chem. Eng. 6 (2018) 2942–2953, https://doi.org/10.1021/acssuschemeng.7b02214.
[72] N. Sebeia, M. Jabli, A. Ghith, T.A. Saleh, Eco-friendly synthesis of Cynomorium coccineum extract for controlled production of copper nanoparticles for sorption of methylene blue dye, Arab. J. Chem. 13 (2020) 4263–4274, https://doi.org/10.1016/j.arabjc.2019.07.007.
[73] E. Vazquez-Velez, L. Lopez-Zarate, H. Martinez-Valencia, Electrospinning of polyacrylonitrile nanofibers embedded with zerovalent iron and cerium oxide nanoparticles, as Cr(VI) adsorbents for water treatment, J. Appl. Polym. Sci. 137 (2020) 1–10, https://doi.org/10.1002/app.48663.
[74] F.A. Ngwabebhoh, N. Mammadli, U. Yildiz, Bioinspired modified nanocellulose adsorbent for enhanced boron recovery from aqueous media: optimization, kinetics, thermodynamics and reusability study, J. Environ. Chem. Eng. 7 (2019), 103281, https://doi.org/10.1016/j.jece.2019.103281.
[75] M. Carballa, G. Fink, F. Omil, J.M. Lema, T. Ternes, Determination of the solid-water distribution coefficient (Kd) for pharmaceuticals, estrogens and musk fragrances in digested sludge, Water Res. 42 (2008) 287–295, https://doi.org/10.1016/j.watres.2007.07.012.
[76] Y.X. Ren, K. Nakano, M. Nomura, N. Chiba, O. Nishimura, A thermodynamic analysis on adsorption of estrogens in activated sludge process, Water Res (2007), https://doi.org/10.1016/j.watres.2007.01.058.
[77] W. Wang, J. Hu, R. Zhang, C. Yan, L. Cui, J. Zhu, A pH-responsive carboxymethyl cellulose/chitosan hydrogel for adsorption and desorption of anionic and cationic dyes, Cellulose 28 (2021) 897–909, https://doi.org/10.1007/s10570-020-03561-4.
[78] J. Han, W. Qiu, Z. Cao, J. Hu, W. Gao, Adsorption of ethinylestradiol (EE2) on polyamide 612: Molecular modeling and effects of water chemistry, Water Res. 47 (2013) 2273–2284, https://doi.org/10.1016/j.watres.2013.01.046.
[79] J. He, Q. Zhou, J. Guo, F. Fang, Characterization of potassium hydroxide modified anthracite particles and enhanced removal of 17α-ethinylestradiol and bisphenol A, Environ. Sci. Pollut. Res. 25 (2018) 22224–22235, https://doi.org/10.1007/s11356-018-2287-5.